

Original Article

Machine learning integrations for development of a T-cell-tolerance derived signature to improve the clinical outcomes and precision treatment of hepatocellular carcinoma

Junjian Li^{1*}, Ji Chen^{2*}, Qiqi Tao², Jianjian Zheng³, Zhenxu Zhou⁴

¹Department of Hepatobiliary Surgery, The First Affiliated Hospital of Wenzhou Medical University, Wenzhou 325000, Zhejiang, P. R. China; ²Key Laboratory of Diagnosis and Treatment of Severe Hepato-Pancreatic Diseases of Zhejiang Province, The First Affiliated Hospital of Wenzhou Medical University, Wenzhou 325000, Zhejiang, P. R. China; ³Key Laboratory of Clinical Laboratory Diagnosis and Translational Research of Zhejiang Province, The First Affiliated Hospital of Wenzhou Medical University, Wenzhou 325000, Zhejiang, P. R. China; ⁴Department of Hernia and Abdominal Wall Surgery, The First Affiliated Hospital of Wenzhou Medical University, Wenzhou 325000, Zhejiang, P. R. China. *Equal contributors.

Received August 22, 2022; Accepted January 7, 2023; Epub January 15, 2023; Published January 30, 2023

Abstract: Hepatocellular carcinoma (HCC) is characterized by high rates of recurrence and metastasis and poor prognosis. A recently discovered concept of T cell tolerance (TCT) has become an entirely new target of cancer immunotherapy. Unfortunately, the effect of TCT on the outcomes of HCC has not been explored. In this study, 7 public datasets and one external clinical cohort, including 1716 HCC patients were explored. Through WGCNA analysis and differential analysis, we explored the key TCT-related modulates. A total of 95 machine learning integrations across all validation cohorts were compared and the optimal method with the highest average C-index value was selected to construct the TCT derived signature (TCTS). In all independent clinical cohorts, TCTS showed accurate prediction of the prognosis, and was significantly correlated with clinical indicators and molecular features. Compared with 77 published gene signatures, the TCTS exhibited superior predictive performance. In the external clinical cohort, a novel nomogram (comprising TNM stage, Hepatitis B, Vascular invasion, Perineural invasion, AFP and TCTS) was constructed to test the clinical performance of TCTS. The results showed that the high TCTS scoring group showed dismal prognosis, improved sensitivity to oxaliplatin and good response to anti-PD-1/PD-L1 immunotherapy. Moreover, the low TCTS score group had few genomic alterations, low immune activation and low PD-1/PD-L1 expression levels. In conclusion, TCTS is an ideal biomarker for predicting the clinical outcomes and improving precision treatment of HCC.

Keywords: Machine learning, hepatocellular carcinoma, T cell tolerance, prognostic signature

Introduction

As the most predominant histological liver cancer subtype, hepatocellular carcinoma (HCC) is the fourth most common cause of cancer-related mortality worldwide [1]. The overall survival (OS) outcomes for HCC patients exhibit global variations, with a median survival time of 2.5 months in sub Saharan Africa, but is significantly higher in developed countries [2]. It is important to effectively identify all adults at risk of HCC using multiple tumor biomarkers (a-feto-protein (AFP), CEA (carcinoembryonic antigen)

and carbohydrate antigen 19-9 (CA199) among others). Advances in artificial intelligence (AI) have provided a unique opportunity for improving the clinical care of HCC patients [3]. As an AI subset, machine learning contributes to efficient curation of electronic health record data, histopathology, and molecular biomarkers by running algorithms that iterate over repeated models [4, 5]. However, current machine learning applications are limited to single algorithms, and cross-sectional comparisons are lacking for clinical treatments.

The main therapeutic options for early-stage HCC include resection, ablation, or transplantation [6]. Traditional systemic therapies are still widely used for patients with intermediate or advanced stage. Assessment of the prognosis and pathologic stage of HCC is extremely important [7]. Immune checkpoint inhibitors (ICIs)-based immunotherapy has also shown strong antitumor activities in HCC patients [8]. With combination of systemic immunomodulation and anti-PD-1/PD-L1 therapy, the immune landscape can effectively be maintained [9]. One of the major challenges in HCC immunotherapy is the discovery and validation of predictive biomarkers for advanced therapy at early stages [10]. As a new platinum-based anticancer agent, oxaliplatin is associated with better survival outcomes than sorafenib in advanced HCC [11, 12]. The synergistic and sustained antitumor effects of combined immune checkpoints and oxaliplatin are significantly superior to either alone [13]. Therefore, there is need to inform on precision treatment of HCC by designing effective biomarkers for simultaneously evaluating responsiveness to immunotherapy and oxaliplatin treatment.

Recently, Michelson et al. reported lineage defining transcription factors for medullary thymic epithelial cell subtypes [14]. Model antigens expressed with the aid of lineage transcription factors are sufficient to induce T cell tolerance (TCT). This finding has informed on exploration of immunotherapy and immune mechanisms for HCC. Li et al. found that PD-1 accumulation and Treg upregulation play a key role in inducing distant immune tolerance in HCC [15]. Determination of relevant indicators for TCT contributes to identification of powerful biomarkers to screen suitable patients for anti-PD-1 combination therapy [16]. Therefore, systematic exploration of transcription factor-related genes has a great potential for promoting HCC immunotherapy.

To bridge the above gaps, we investigated the clinical implications of TCT in HCC based on machine learning integrations. With the aid of 8 independent clinical cohorts and 95 machine learning integrations, an efficient TCT derived signature was constructed to improve the prognosis, clinical decision making, immunotherapy, and oxaliplatin treatment of HCC.

Materials and methods

Data preparation

Eight independent clinical cohorts (TCGA, ICGC, GSE116174, GSE54236, GSE76427, GSE14520, GSE27150 and FAHWMU) containing 17-16 HCC patients were included in this study. The criteria for identification of clinical cohorts from public database were: I. Cohorts with more than 50 samples with survival information; II. At least 10,000 clearly annotated genes; and III. Cohorts including patients with no other treatments before resection. Entire genomic profiles and relevant clinical characteristics for HCC patients in the TCGA cohort were downloaded from the Genomic Data Commons (<https://portal.gdc.cancer.gov/>). Transcriptome data were normalized based on Fragments Per Kilobase of exon model per Million mapped fragments (FPKM). The FAHWMU cohort was selected from the First Affiliated Hospital of Wenzhou Medical University (FAHWMU) (Wenzhou, China). The human research ethics committee of the First Affiliated Hospital of Wenzhou Medical University approved this study. All patients/participants were required to sign a written informed consent and were all treated with a standard systemic therapy. The inclusion criteria for patients were: I. Those aged 18 years or older; II. Those with good hematological and renal functions; III. Determination of HCC was according to response evaluation criteria of solid tumors (RECIST, version 1.1) and IV. Those whose oncology group status of 0 and 1 were explicit. For the FAHWMU cohort, gene expression profiles were obtained based on quantitative real-time PCR (qRT-PCR). Laboratory variables (e.g., Hepatitis B, a-fetoprotein (AFP), carcinoembryonic antigen (CEA) and carbohydrate antigen 19-9 (CA199)) were assessed from results of a test that was closest to the surgical date. The TNM stage for each HCC patient was assessed based on the 8th edition of the AJCC Staging Manual. Histopathological variables (e.g., tumor size, lymph node invasion, vascular invasion, and perineural invasion) were also included. Descriptive statistics for clinical characteristics in the FAHWMU cohort are shown in [Table S1](#). The ICGC cohort was obtained from the ICGC data portal (<https://dcc.icgc.org/projects/LIRI-JP>). The other clinical cohorts (GSE116174, GSE54236, GSE76427, GSE14520, and GSE27150) were

A novel T-cell-tolerance derived signature

downloaded from the Gene Expression Omnibus (GEO) database (<https://www.ncbi.nlm.nih.gov/geo/>). Among them, the GSE116174 cohort was retrieved from the Affymetrix HT HG-U133+ PM Array Plate platform; the GSE54236 cohort was retrieved from the Agilent-014850 Whole Human Genome Microarray 4x44K platform [17]; the GSE76427 cohort was retrieved from the Illumina HumanHT-12 V4.0 expression beadchip platform [18]; the GSE14520 cohort was retrieved from the Affymetrix Human Genome U133A 2.0 Array platform [19] while the GSE27150 cohort was retrieved from the State Key Lab Homo sapien 2.6 K platform. Signatures of lineage-defining transcription factors in distinct medullary thymic epithelial cell subtypes were obtained from a previous study [20]. As described in the study, lineage-defining transcription factors can effectively induce T cell tolerance by driving mimetic cell accumulation. Therefore, these lineage-defining transcription factors can be used to assess the T cell tolerance landscape, and their downstream genes are potential TCT-related genes. The downstream genes of these transcription factors were selected using the Cistrome Data Browser (<http://cistrome.org/db/#/>).

Quantitative real-time PCR

For the FAHWMU cohort, total RNA from HCC tissues of each patient was extracted using the Trizol reagent. Then, the RNA was reverse transcribed into cDNA using the ribo scripttm reverse transcription kit. With the aid of glyceraldehyde 3-phosphate dehydrogenase (GAPDH), RNA expressions were calibrated. Real-time PCR was performed on a 7500 fast quantitative PCR system (Applied Biosystems, USA) using the SYBR Green master mix. The CT value for each well was recorded, and it was calculated using the $2^{-\Delta CT}$ method.

Consensus clustering

Consensus clustering was performed using the “ConsensusClusterPlus” R package to group the HCC patients into main TCT-related subtypes [21]. The consensus cumulative distribution function (CDF) curve was established based on the consensus index and CDF slopes. We hypothesized that the consensus index value was transformed from 0.1 to 0.9. Then, slopes of CDF curves were compared, and the one with the smallest slope determined as the

optimal value to separate the TCT-related subtypes [22].

Evaluation of immune infiltration

The CIBERSOFT algorithm was used to determine the relative contents of 22 tumor immune infiltrating cells (TIICs). As an analytical tool developed by Newman et al. in the Alizadeh lab, the CIBERSOFT algorithm is used to estimate the abundance of member cell types in mixed cell populations using gene expression profiles (<https://cibersortx.stanford.edu/>) [23]. To verify the findings from the CIBERSOFT algorithms, we calculated the relative scales of fractions of 17 immune cells and 13 immune related pathways using the “GSVA” R package. To precisely assess tumor cell proportions as well as the infiltrating immune and stromal cells, Estimation of STromal and Immune cells in MAlignant Tumour tissues using Expression data (ESTIMATE) algorithm was used based on the online website (<https://bioinformatics.mdanderson.org/estimate/index.html>). Based on the differential transcripts, we applied the GO (gene ontology) database for functional annotation enrichment analysis (including biological process, cellular component and molecular function) (<http://pantherdb.org/>).

Weighted gene co-expression network analysis (WGCNA)

In this study, WGCNA was performed to identify potential gene sets with similar TCT-related expression patterns and to screen the key regulatory genes. The WGCNA steps were: I. The correlation coefficients were calculated based on expression patterns between different TCT related clusters; II. By delineating genes with close correlation in the co-expression network, a threshold was established to partition into different patterns; and III. By performing comparisons between TCT clusters and biological pathways, the threshold with the highest coefficient to TCT clusters was selected to determine the key TCT related patterns.

Construction of optimal TCTS

Ten machine learning algorithms (Lasso, Logistic, Ridge, Stepwise Cox, Random Forest (RF), Cox Boost, Survival Support Vector Machine (SVM), generalized boosted regression modeling (GBM), elastic network (Enet) and

A novel T-cell-tolerance derived signature

supervised principal components (SuperPC)) were transformed into 95 kinds of machine learning integrations. The 10 machine learning algorithms are described: I. The Ridge, Logistic, Lasso and Enet regression analyses were performed using the “glmnet” R package. Based on 10-fold cross validation, the leave one out cross validation framework was constructed to obtain the optimal regularization parameter (λ). With λ 's segmentation, the signature was further compressed and correlation coefficients determined. For Enet regression analysis, the regularization parameter was selected based on the leave one out cross validation framework, while the L1-L2 tradeoff was set to 0.1-0.9 (interval = 0.2); II. Using the “survival” R package, the stepwise Cox algorithm was constructed using the Akaike information criterion (AIC). The “simultaneous”, “backward”, and “forward” were all treated as orientation modes to perform the stepwise Cox regression analysis. The key prognostic genes and relevant correlation coefficients were finally determined by stepwise compression regression; III. The Random Forest (RF) plot was established using the “randomforest” R package. The RF had two different parameters (nTree and mtry). The mtry was the number of variables that had been randomly selected at each node for splitting, while nTree denoted the number of trees in the forest. In the RF regression analysis, all pairs of nTree and mtry were obtained. The combination of nTree and mtry with the highest C-index value was determined as the optimization parameter. Therefore, the optimal genes and regression coefficients were divided; IV. Cox Boost was implemented using the “coxboost” R package to fit the Cox proportional hazards model through component likelihood boosting; V. The Survival SVM regression method was based on support vector regulation and enabled the prediction of survival time and status through covariates; VI. The GBM regression analysis was achieved using the “superpc” R package. According to the leave one out cross validation framework and cv.gbm, the index with the smallest cross validation error number tree was selected to determine the boosted regression signature; VII. Through principal component analysis, SuperPC regression analysis was performed using the “superpc” R package. It generated a linear capture based on maximum direction of the feature or combination of variables of interest. Then, the cv.

function used a form of leave one out cross validation framework to estimate the supervised optimal feature thresholds in principal components. The “pre-validation approach” was performed to avoid challenges associated with small validation cohorts.

Construction of the optimal TCTS was done as: I. Univariate Cox regression analysis was performed to identify the significantly expressed prognosis-related TCT related modulates; II. Ten machine learning algorithms were transformed into 95 kinds of machine learning integrations; III. Machine learning integrations were first performed based on prognosis related TCT-related modulates in the TCGA cohort; IV. In the other clinical validation cohorts, the machine learning integrations were used to obtain the individual C-index value; IV. The machine learning integration with the highest average C-index value across all clinical cohorts was determined as the optimal one to construct the TCTS.

Immunohistochemistry (IHC) staining images

In this study, immunohistochemistry (IHC) staining images were obtained. First, paraffin-embedded tissue sections of HCC were sliced into 4 μm -thick sections. Then, the tissue sections were deparaffinized, rehydrated, microwaved for antigen retrieval, and subjected to hydrogen peroxide blocking to reduce non-specific background staining. The sections were sealed with 10% serum for 1 h at 37°C. Then, the sections were incubated with anti-PD-1 or PD-L1 antibodies overnight. The following day, samples were incubated with a primary antibody enhancer and HRP polymer. Finally, specific binding sites were established by DAB staining.

Immunotherapy and drug sensitivity analysis

The Wolf cohort 2021 (Anti-PD-L1), Ascierto cohort 2016 (Anti-PD-1), Homet cohort 2019 (Anti-PD-1) and Amato cohort 2020 (Anti-PD-1) were all included in this study. They were obtained from the GSE173839, GSE67501, GSE111636 and GSE145996 cohorts, respectively. Drug sensitivity analysis of Oxaliplatin was performed using the Genomics of Drug Sensitivity in the Cancer-2 (GDSC2) database (<https://www.cancerrxgene.org/>). Cell viabilities under the influence of Oxaliplatin were

A novel T-cell-tolerance derived signature

determined using the metabolic assay (resazurin/celltiter glo). Tolerability was determined using the half maximal inhibitory concentration (IC50).

Statistical analysis

All bioinformatics analyses were performed using R 4.2.1 (<https://www.r-project.org/>). The statistical class graphs were plotted using the Graphpad Prism (<https://www.graphpad-prism.com/>). For cohorts with small sample sizes ($n < 50$), the t-test was used for differential analysis. For the other cohorts, the Wilcoxon test was used for differential analysis, guaranteeing that it does not depend on probability distribution belonging to any particular parameter. Time dependent ROC curves were constructed using the 'timeROC' R package. The nomogram and calibration curves were generated using the "rms" R package. All p values were two tailed and $P < 0.05$ was the threshold for statistical significance.

Results

Identification of key TCT-related modulates

As shown in the flow diagram (**Figure 1**), the overall design can be described as. I. Identification of key TCT derived modulates; II. Construction of optimal TCTS; III. Clinical implication value of TCTS was correlated with clinical traits, pathological index and molecular features; IV. Prognostic capacity of the TCTS was compared with 77 published gene signatures; v. The IHC staining images and immune landscapes were used to verify the potential immunotherapeutic implications of TCTS; and VI. Further clinical implications of TCTS were determined. In the TCGA cohort, consensus clustering was implemented based on genomic profiles of TCT-related genes to screen for potential TCT-derived subtypes. With the consensus k value from 2 to 9, we selected $k = 4$, with the smallest CDF slope, to determine the clusters (**Figure 2A**). **Figure 2B** shows the distributions of HCC patients when consensus matrix $k = 4$. In **Figure S2A**, the complex heatmap plotted the distribution of clinical traits, TIICs and ESTIMATE scores between different clusters. These findings indicate that ESTIMATE scores were enriched in clusters 1 & 2. Moreover, the abundances of CD8 T cells, activated memory CD4 T cells and follicular helper T cells were sig-

nificantly high in cluster-2. Macrophages of the M2 phenotype were enriched in cluster-3 while M0 macrophages were enriched in cluster-4. To verify the results in the CIBERSOFT algorithm, ssGSEA analysis was performed. Relative abundances of immune cells (**Figure 2C**) and immune-related pathways (**Figure 2D**) were markedly high in TCT-related cluster-2 ($P < 0.01$), and significantly low in cluster-3 ($P < 0.05$). Correlations between ESTIMATE scores and TCT-related clusters were also validated (**Figure 2F**, $P < 0.001$). In WGCNA analysis of TCT-related clusters, the soft threshold was determined as 5 to construct the optimal network (**Figure S1**). In **Figure 2E**, MEblue was determined as the key TCT-related pattern. Then, GO enrichment analysis revealed that genes in MEblue were highly enriched in immune activation (T cell activation, and leukocyte mediated immunity among others) associated biological functions (**Figure S2B**). Then, differential analysis was performed to screen for significantly differentially expressed genes (DEGs) among the TCT-related clusters ($|\text{LogFC}| > 2$; $P < 0.001$). The venn diagram revealed that 252 intersection genes were obtained as key TCT-derived modulates by intersecting genes within WGCNA analysis and differential analysis (**Figure 2G**). The 252 intersection genes are presented in **Table S2**.

Construction of optimal TCTS

A total of 145 prognosis-related TCT derived genes were screened via univariate Cox regression analysis. Then, 95 machine learning integrations were used to construct the TCTS across 8 independent clinical cohorts individually. In **Figure 3A**, the one with the highest average C-index value (Lasso + stepCox) was determined as the optimal integration to generate the TCTS. In Lasso regression analysis, the optimal λ and distribution of coefficients are shown in **Figure 3B, 3C**. The optimal 5 TCT-derived genes and relevant coefficients were obtained via stepCox regression analysis (**Figure 3D**). The K-M survival curves preliminarily revealed that the OS for HCC patients in the high TCTS scoring group was significantly dismal when compared to the low TCTS scoring group in all clinical cohorts (**Figure 3E**).

Clinical prognostic performance of TCTS

The time-dependent ROC analysis was performed to verify the prognostic value of TCTS in

A novel T-cell-tolerance derived signature

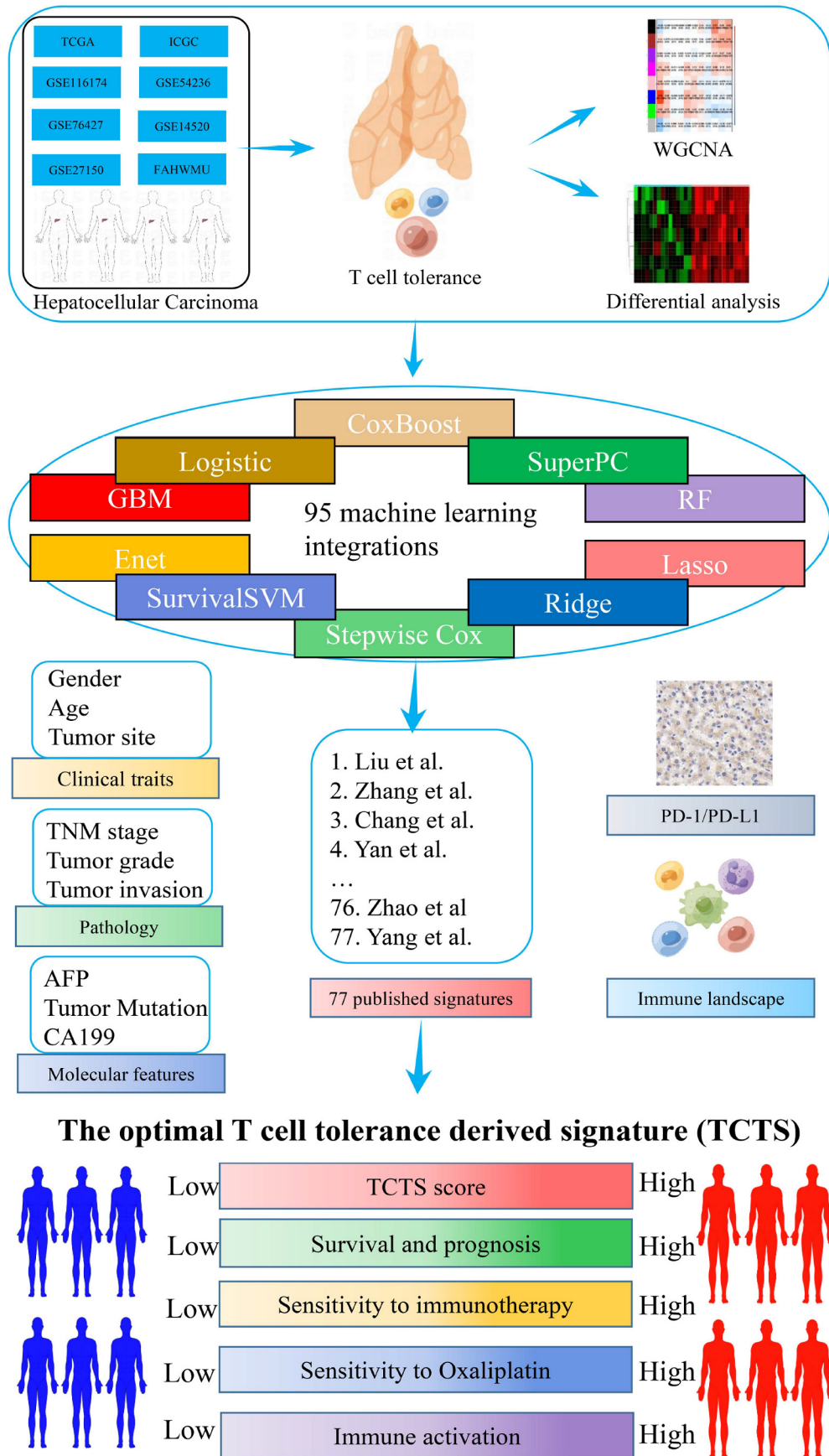


Figure 1. A flow diagram showing the overall design of the study.

A novel T-cell-tolerance derived signature

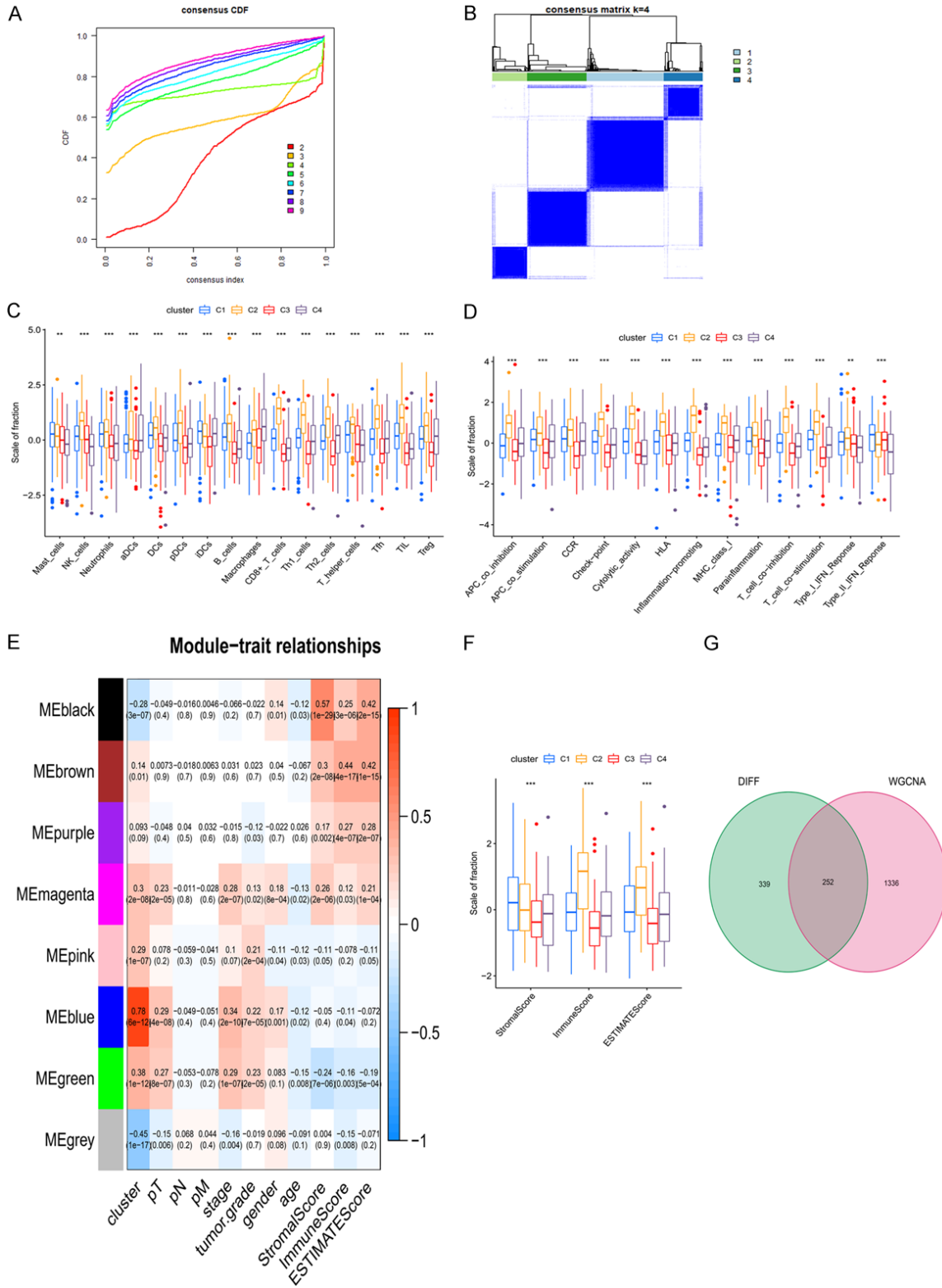


Figure 2. Identification of key TCT-related modules in the TCGA cohort. (A) Consensus CDF curves with the k value from 2 to 9. (B) The distribution of HCC patients in the consensus clustering when k = 4. (C, D) The boxplot showing differences in the scale of fraction of 17 immune cells (C) and 13 immune related pathways (D) between different TCT related clusters. (E) WGCNA showing the associations among potential TCT-related patterns, TCT-related clusters, clinical characteristics, tumor mutation burden and ESTIMATE scores. (F) The boxplot displaying differences in Immune score, Stromal score, and ESTIMATE score between different TCT-related clusters. (G) The Venn diagram illustrating the intersection genes between WGCNA and differential analysis.

A novel T-cell-tolerance derived signature

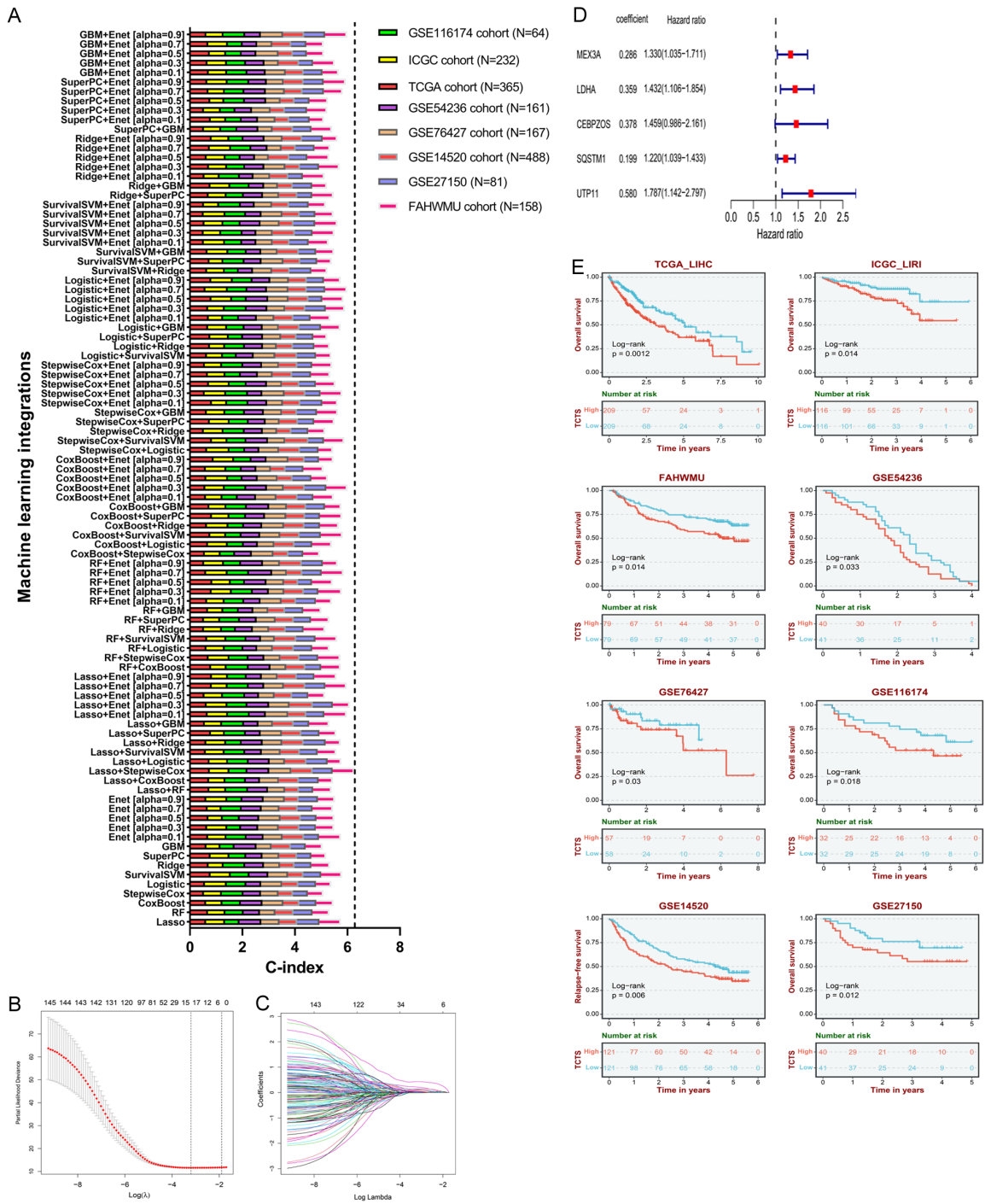
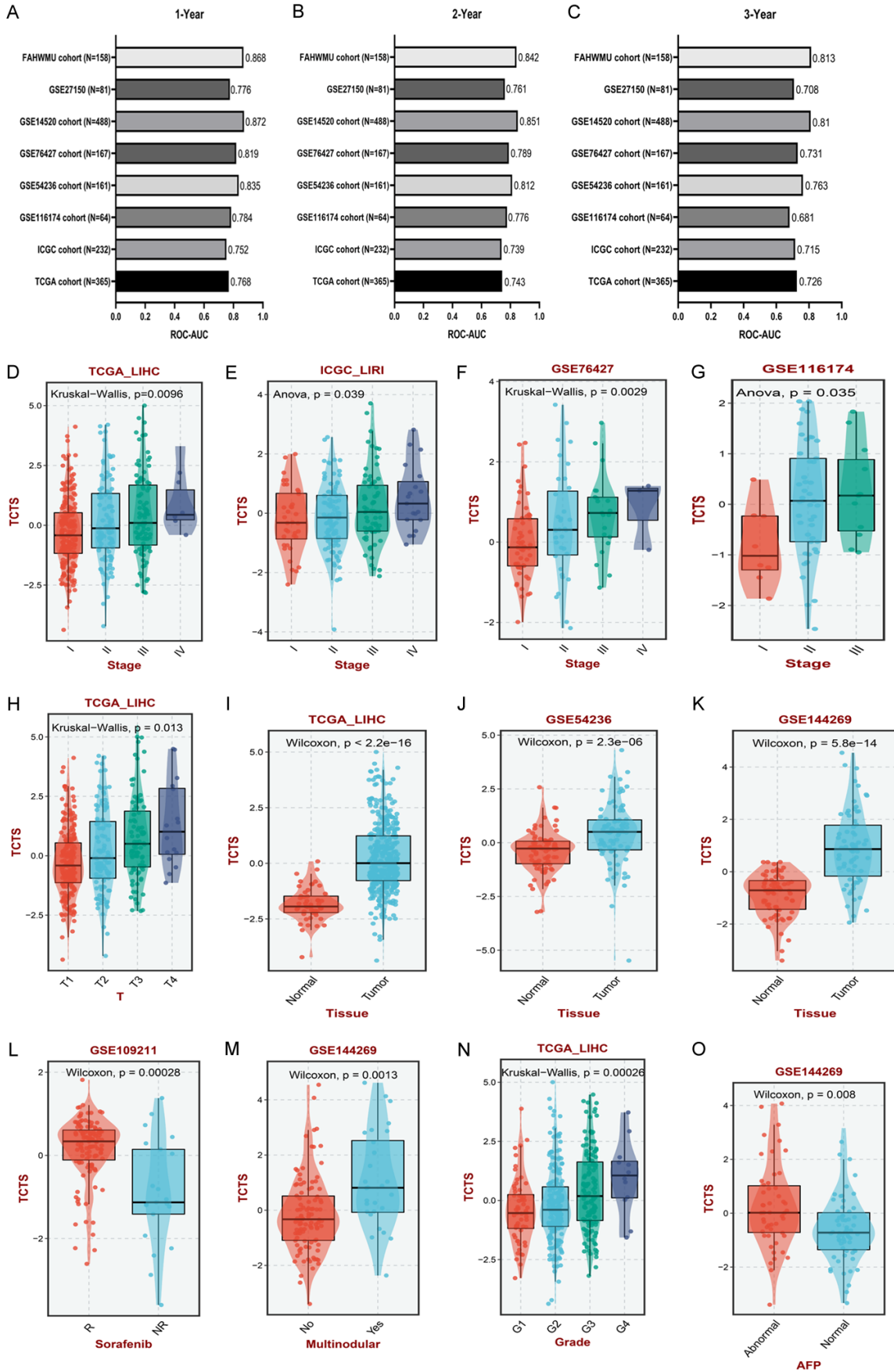


Figure 3. Construction of the optimal TCT derived signature. **A.** The comparison of 95 machine learning integrations across all independent clinical cohorts. **B.** Determination of the optimal λ , when the partial likelihood deviance reached the minimum value in the Lasso regression analysis. **C.** The correlation between $\log \lambda$ and coefficient across all prognostic TCT related modulates. **D.** A forest plot showing the coefficient and Hazard ratio for each TCTS gene in the stepwise Cox regression analysis. **E.** K-M survival curves illustrating the difference in OS between low TCTS scoring group and high TCTS scoring group in all independent clinical cohorts (all $P < 0.05$).

HCC. The ROC-AUC values for the 1st year were 0.868, 0.776, 0.872, 0.819, 0.835, 0.784,

0.752 and 0.768 in each cohort (**Figure 4A**); those of the 2nd-year were 0.842, 0.761, 0.851,

A novel T-cell-tolerance derived signature



A novel T-cell-tolerance derived signature

Figure 4. The clinical prognostic value of TCTS. (A-C) The AUC value of ROC curves for all independent clinical cohorts in the 1st (A), 2nd (B) and 3rd (C) years. (D-G) The distribution of TCTS scores between different TNM stage groups in the TCGA cohort (D), ICGC cohort (E), GSE76427 cohort (F) and GSE116174 cohort (G). (H) The distribution of TCTS scores between different T stage groups in the TCGA cohort. (I-K) The distribution of TCTS scores between normal tissues and tumor tissues in the TCGA cohort (I), GSE54236 cohort (J) and GSE144269 cohort (K). (L) The distribution of TCTS scores between different sorafenib response groups in the GSE109211 cohort. (M) The distribution of TCTS scores between different multinodular groups in the GSE144269 cohort. (N) The distribution of TCTS scores between different tumor grade groups in the TCGA cohort. (O) The distribution of TCTS scores between different AFP status in the GSE144269 cohort.

0.789, 0.812, 0.776, 0.739 and 0.743 in each cohort (**Figure 4B**) while those of the 3rd-year were 0.813, 0.708, 0.81, 0.731, 0.763, 0.681, 0.715 and 0.726 in each cohort (**Figure 4C**). In clinical cohorts with pathological stage (including TCGA, ICGC, GSE76427 and GSE116174 cohorts), the TCTS score was positively correlated with pathological stage (**Figure 4D-G**, $P < 0.05$). In other pathological indicators, including T stage, multinodular and tumor grade, the TCTS score exhibited comparable findings (**Figure 4H, 4M** and **4N**, $P < 0.05$). In tissue differentiation, TCTS showed a great ability to distinguish between tumor and normal tissues (**Figure 4I-K**, $P < 0.05$). Correlations between Sorafenib response, AFP status and TCTS were also plotted (**Figure 4L** and **4O**, $P < 0.05$). In **Figure 5**, we compared the C-index value between TCTS and 77 published gene signatures. Details of the 77 published signatures are provided in [Table S3](#). In most independent clinical cohorts (including TCGA, GSE54236, GSE76427, GSE14520 and FAHWMU cohorts), the C-index values for our TCTS (0.759, 0.835, 0.84, 0.813 and 0.829, respectively) were significantly superior than those of the other published gene signatures. In the ICGC cohort, the signature of Tao et al. (C-index = 0.751) was more effective in predicting prognosis than TCTS (C-index = 0.742). In the GSE27150 cohort, the C-index value of TCTS (0.761) was relatively lower compared to those obtained by Deng M (0.765), Zhang Z (0.766), and Zhang Q (0.766). In the GSE116174 cohort, the prognostic value of TCTS was relatively suboptimal (C-index = 0.684). In summary, in most independent clinical cohorts, the C-index value of our TCTS was higher when compared with those of 77 published gene signatures, suggesting the superior prognostic prediction capacity of TCTS.

Construction of a novel nomogram in the external clinical cohort

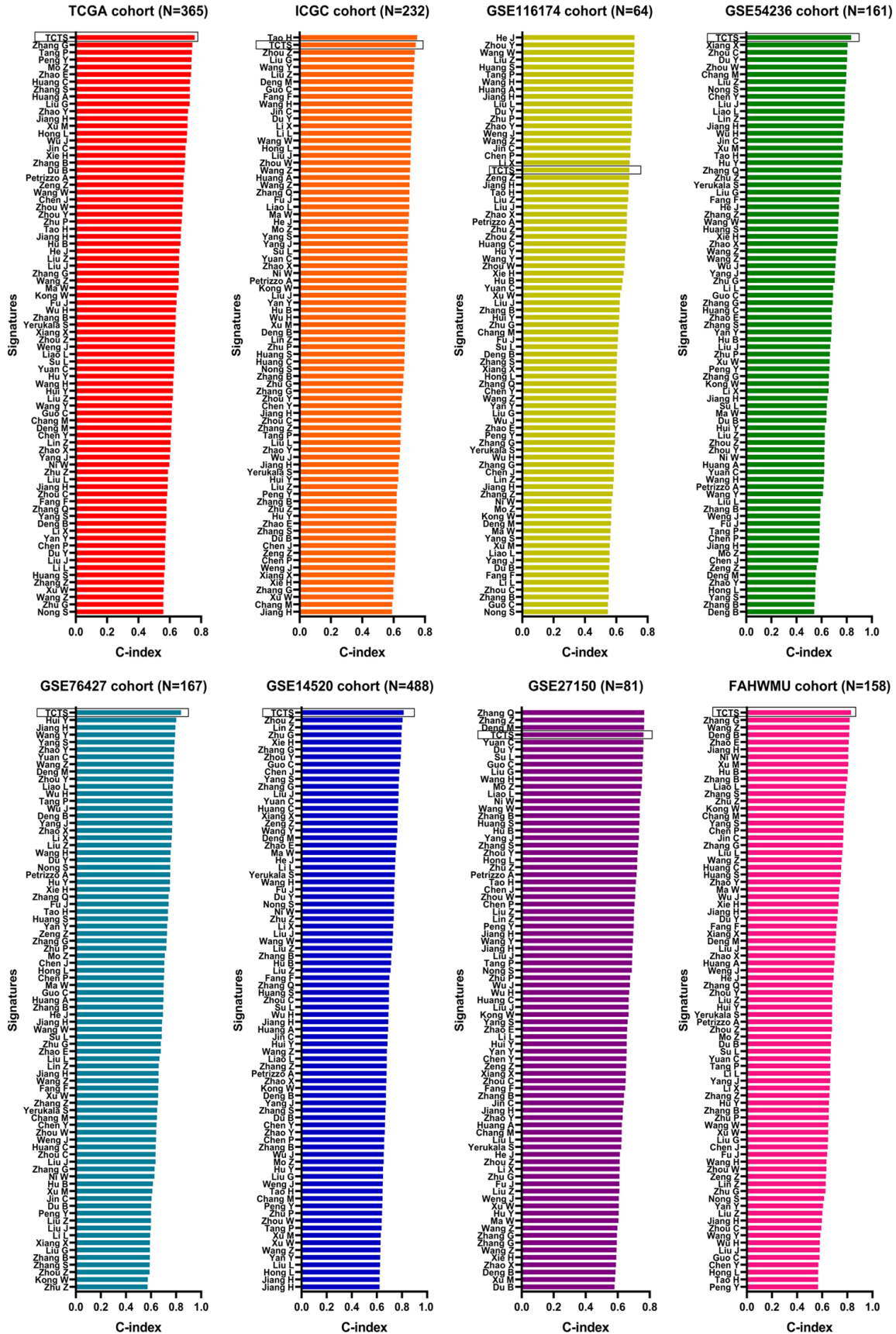
To elucidate on the clinical implications of TCTS, we used a combination of TCTS, physical exam-

ination data (age, gender), pathological indicators (TNM stage, tumor size, Hepatitis B, lymph node invasion, vascular invasion, perineural invasion, albumin) and molecular features (AFP, CEA, CA199). In the FAHWMU cohort, the complex ROC curves revealed the ROC-AUC values of clinical traits. Albumin had the highest AUC value (0.735) while lymph node invasion had the lowest value (0.502) (**Figure 6A**). Univariate Cox analysis revealed the individual impact of each clinical trait on prognostic prediction (**Figure 6B**). Multivariate Cox analysis showed the combined value of all clinical traits and TCTS in prognostic prediction (**Figure 6C**). It was established that TNM stage, Hepatitis B, vascular invasion, perineural invasion AFP and TCTS were relatively more robust in terms of prediction ($P < 0.05$). Clinical applicabilities of these indicators were assessed using the nomogram (**Figure 6D**). As proven by the calibration curves, the nomogram can predict the 1st, 2nd and 3rd year prognostic outcomes (**Figure 6E**).

Potential molecular mechanisms of TCTS

In **Figure 7A**, the boxplot shows the distributions of TILCs between low- and high-TCTS score groups. It is shown that CD8 T cells, resting memory CD4 T cells, Tregs, M1 macrophages and ESTIMATE scores were highly enriched in the high-TCTS score group ($P < 0.05$) while M0 macrophages, M2 macrophages, and resting mast cells were significantly enriched in the low-TCTS scoring group. The GSEA-GO enrichment analysis revealed that high-TCTS score groups were enriched in biological pathways such as replication, apoptosis and immunity (**Figure S3A**). The distributions of genomic alterations between low- and high-TCTS score groups are shown in **Figure S3B**. These findings show that relative levels of TP53 and several loss predominant point mutations were significantly high in the high-TCTS score group. The IHC staining images showed that PD-1/PD-L1 expressions were markedly elevated in the

A novel T-cell-tolerance derived signature



A novel T-cell-tolerance derived signature

Figure 5. Comparison of C-index between TCTS and 77 published gene signatures in all independent clinical cohorts. Comparison of the C-index between TCTS and 77 published gene signatures based on the following steps: (1) A total of 77 published gene signatures of HCC were obtained from published articles; (2) The risk score of an individual gene signature was calculated using a formula provided in previous articles; (3) The C-index value of TCTS and published gene signatures in all independent clinical cohorts were calculated using the R package “compareC”; (4) In each independent clinical cohort, the C-index value between TCTS and 77 published gene signatures were compared. One with the highest C-index value was considered to have superior predictive capacity.

high-TCTS score group (**Figure 7B-E**). **Figure 8A-D** shows that the TCTS scores can effectively predict the responses of immune checkpoint inhibition (ICIs) in four independent immunotherapeutic cohorts (Wolf cohort 2021, Ascierto cohort 2016, Homet cohort 2019, and Amato cohort 2020). The subsequent ROC curves verified the predictive capacity of TCTS (AUC = 0.686 in the Wolf cohort 2021, AUC = 0.929 in the Ascierto cohort 2016, AUC = 0.733 in the Homet cohort 2019 and AUC = 0.688 in the Amato cohort 2020) (**Figure 8E-H**). Agent sensitivity analysis revealed that TCTS was significantly correlated with the IC50 of oxaliplatin in the TCGA, ICGC, GSE76427, GSE54236, GSE27150 and GSE14520 cohorts, respectively (**Figure 8I-N**).

Discussion

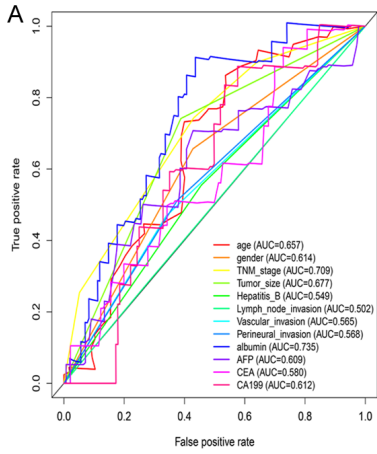
As a result of delayed diagnosis and limited efficacies of existing therapies, the 5-year survival rate for HCC patients is low [24]. Liver transplantation for the vast majority of patients is limited by insufficient medical resources [25]. Meanwhile, traditional staging systems (e.g., TNM stage, and BCLC stage) have not met the needs of precision medicine in assessing prognosis and liver dysfunctions in advanced HCC [26]. Therefore, it is essential to identify novel biomarkers in patients with established HCC to improve the early diagnosis, treatment responses and OS outcomes. Electronic health records data, imaging modalities and histopathology have been widely used as biomarkers for identification of HCC [27, 28]. At the molecular level, various genetic signatures have also been used as novel HCC biomarkers [29]. However, due to wide heterogeneous factors and pathogenesis of HCC, the capacity of these biomarkers for precise prognostic assessment is extremely limited. Advances in AI provide unique opportunities for precision medicine in HCC [30]. As a key AI component, machine learning progressively improves biomarker performance by iterating over the model and optimizing the param-

eters via incorporating additional validation cohorts [31]. Therefore, machine learning can effectively ensure the superiority and robustness of prognostic markers. We compared the performance of 95 machine learning approaches using 8 independent clinical cohorts and determined the optimal one to construct the TCTS. The constructed TCTS exhibited the ability to precisely evaluate the prognostic outcomes. Moreover, exchange of TCTS score were positively associated with pathological stage, tumor grade, sorafenib response and AFP status.

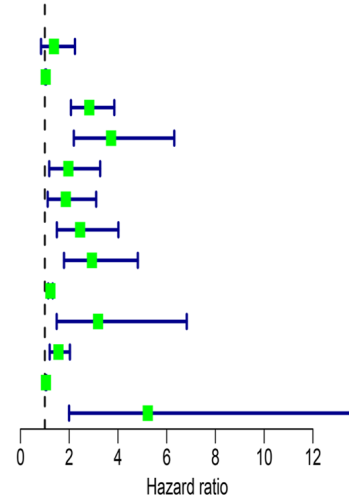
To identify biomarkers for efficient prediction of HCC prognosis and guide target treatment from genomics aspects, various gene signatures were constructed. Xu et al. reported a novel Jab1/CSN5 derived lncRNA signature to improve the clinical outcomes of HCC [32]. Fu et al. constructed a DNA methylation derived signature for prognostic prediction of hepatitis positive HCC [33]. These genetic signatures provide guidance for clinical care of HCC via partial biological function pathways. However, most signatures typically only use one single regression algorithm (e.g., Lasso, stepwise Cox, etc.), therefore, it is difficult to guarantee their efficiency [34, 35]. Various studies focused on machine learning algorithms to construct the signature, but it confined solely to some separate machine learning algorithm (e.g., survival SVM, RandomForest, etc.) [36, 37]. Due to the lack of cross-sectional comparisons of machine learning models, or insufficiency of validation cohorts, most of the current models do not fully satisfy the requirements for precise prediction of HCC. In this study, 95 machine learning integrations were performed using 8 independent clinical cohorts to ensure the superiority and robustness of the signature to the greatest extent.

It has been reported that TCT plays a key inflammation-associated role in fibrosis and HCC development, therefore, targeting TCT interac-

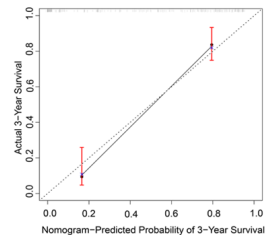
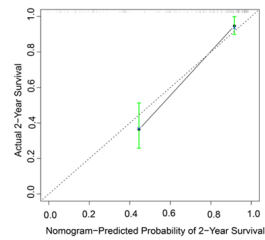
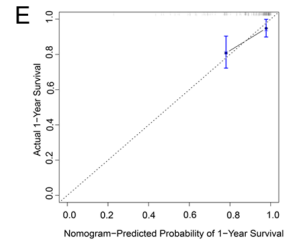
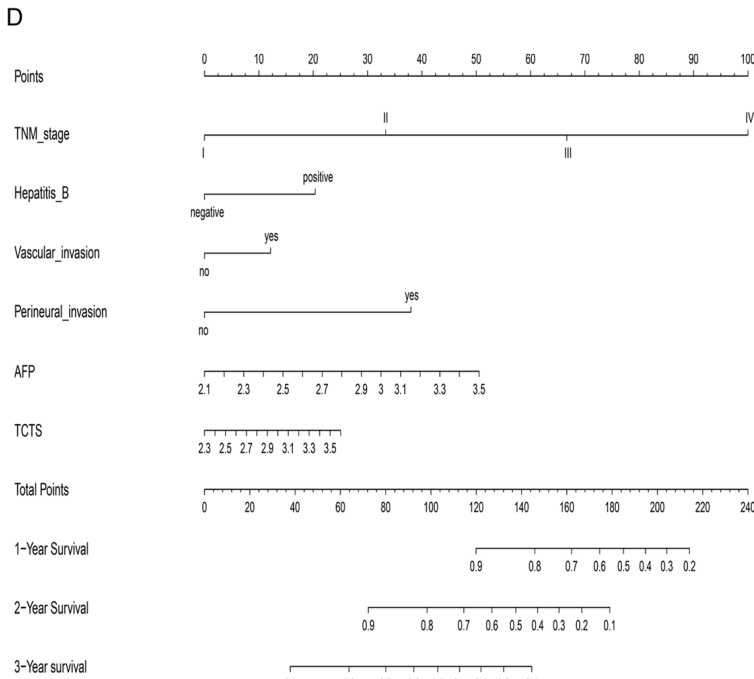
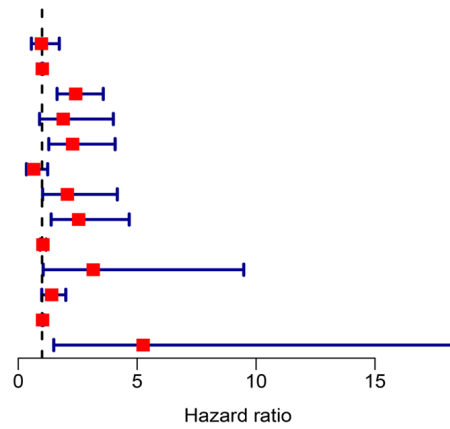
A novel T-cell-tolerance derived signature



	pvalue	Hazard ratio
gender	0.203	1.373(0.843-2.236)
Age	0.003	1.033(1.011-1.055)
TNM_stage	<0.001	2.824(2.071-3.851)
Tumor_size	<0.001	3.718(2.190-6.312)
Hepatitis_B	0.009	1.965(1.180-3.270)
Lymph_node_invasion	0.018	1.861(1.115-3.107)
Vascular_invasion	<0.001	2.448(1.492-4.019)
Perineural_invasion	<0.001	2.931(1.785-4.815)
albumin	<0.001	1.227(1.139-1.322)
AFP	0.003	3.183(1.485-6.824)
CEA	<0.001	1.558(1.198-2.027)
CA199	<0.001	1.045(1.024-1.067)
TCTS	<0.001	5.224(1.994-13.685)

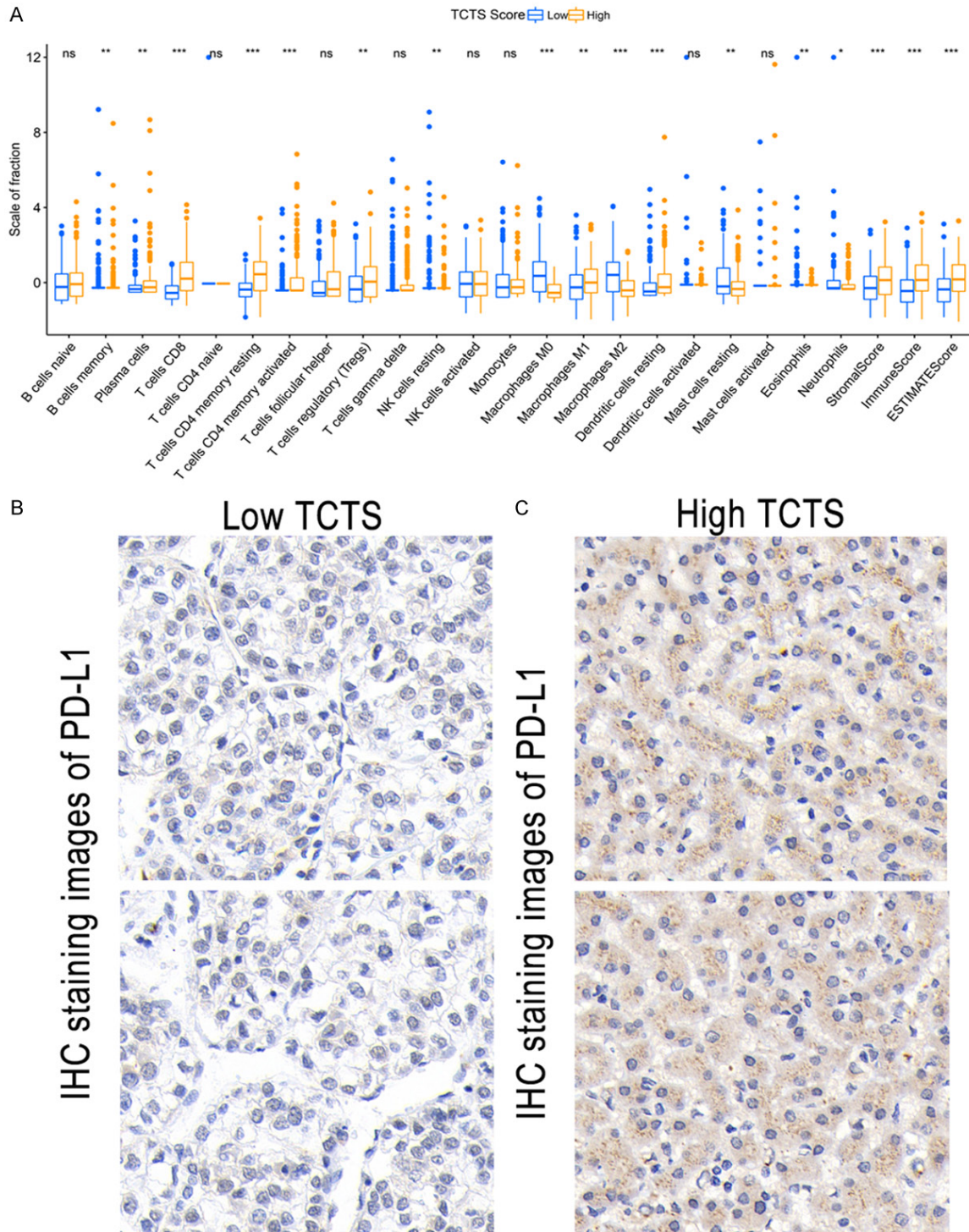


	pvalue	Hazard ratio
gender	0.931	0.975(0.551-1.725)
Age	0.417	1.011(0.985-1.037)
TNM_stage	<0.001	2.414(1.631-3.575)
Tumor_size	0.096	1.891(0.894-3.998)
Hepatitis_B	0.005	2.286(1.283-4.074)
Lymph_node_invasion	0.189	0.651(0.343-1.236)
Vascular_invasion	0.043	2.065(1.024-4.165)
Perineural_invasion	0.003	2.540(1.383-4.665)
albumin	0.553	1.037(0.919-1.171)
AFP	0.041	3.151(1.047-9.482)
CEA	0.059	1.404(0.987-1.999)
CA199	0.136	1.021(0.994-1.049)
TCTS	0.010	5.251(1.492-18.476)



A novel T-cell-tolerance derived signature

Figure 6. The clinical implication of TCTS in the FAHWMU cohort. A. The ROC curves showing the AUC value of clinical characteristics and molecular features in the FAHWMU cohort. B. The univariate Cox regression analysis results showing the impact of the clinical characteristics, molecular features and TCTS in predicting the prognosis. C. The multi-Cox displaying the prognosis prediction performance of clinical characteristics, molecular features and TCTS. D. A nomogram comprising TNM stage, Hepatitis B, Vascular invasion, Perineural invasion, AFP and TCTS for predicting the prognosis. E. The calibration curves of the nomogram in predicting outcomes at 1st, 2nd and 3rd years.



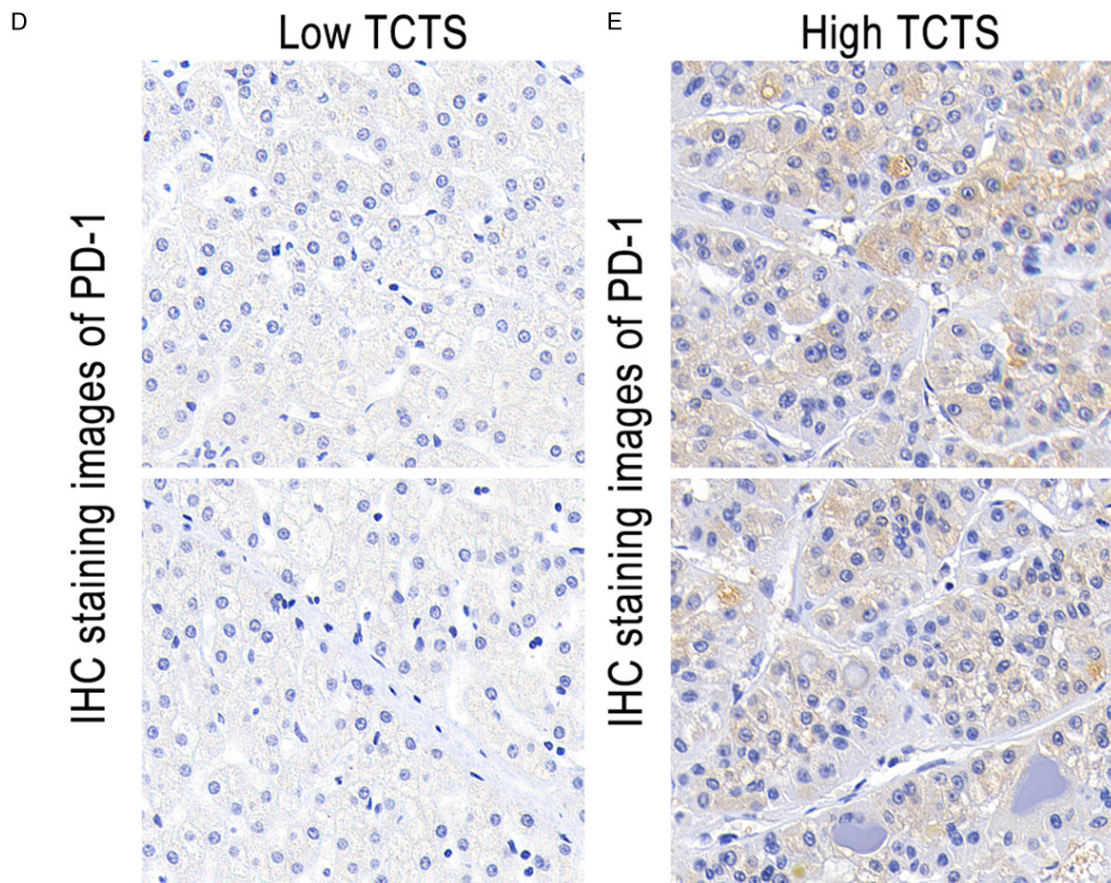


Figure 7. The correlation between TCTS and potential molecular mechanisms. A. The distribution of 22 TIICs and ESTIMATE scores between different TCTS scoring groups (ns: no significant; *: $P < 0.05$; **: $P < 0.01$; ***: $P < 0.001$). B-E. The IHC staining images demonstrated the relative expression levels of PD-1/PD-L1 between High- and Low-TCTS scoring groups.

tions holds great potential in therapy [38, 39]. In this study, a TCT derived signature was constructed and its clinical implications determined. It was found that TCTS could markedly inform on prognosis, immune activation, immunotherapy, and agent treatment of HCC. The CD4 T cells mainly function to remove senescent hepatocytes and alleviate inflammatory responses [40] while the CD8 T cells mainly exert anti-tumor effects in association with IFN [41]. The anti-PD-L1 therapy effectively promotes CD8 T cell infiltrations in tumor environments [42]. Expressions of PD-L1 on infiltrating tumor-associated macrophages can exacerbate the suppression of CD8 T cells in HCC [43]. Our signature exhibited a significant capacity for assessment of T cells and PD-1/PD-L1, which may improve the applications of precision immunotherapy in HCC. The inclusion of 4 immunotherapeutic cohorts validated the

high efficacy and applicability of TCTS. Ding et al. reported that the combination of oxaliplatin with autophagic inhibitors enhances chemotherapeutic efficacies and improves the prognostic outcomes of HCC patients [44]. Wu et al. found that TP53 mutations can significantly enhance tumor invasion and are associated with poor prognostic outcomes of HCC patients [45]. Therefore, TCTS is a powerful tool for assessment of genomic alterations and oxaliplatin responses.

This study has some limitations. First, the biological functions of 5 genes in TCTS were not experimentally validated. Second, clinical trials should be included at follow-up to validate the guiding role of TCTS for immunotherapy and oxaliplatin treatment. Additionally, clinical applicabilities of TCTS should be further validated in larger clinical cohorts.

A novel T-cell-tolerance derived signature

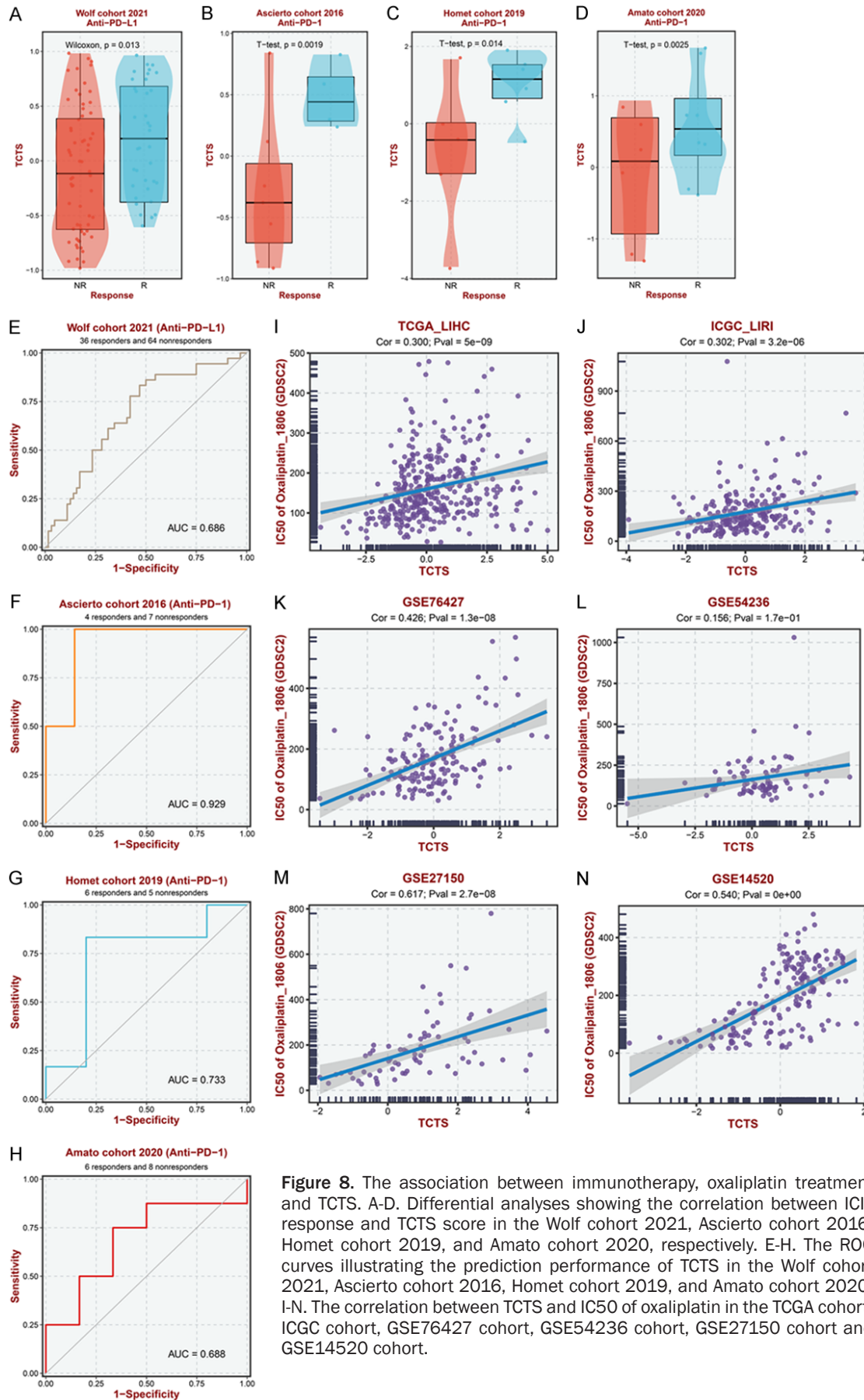


Figure 8. The association between immunotherapy, oxaliplatin treatment and TCTS. A-D. Differential analyses showing the correlation between ICIs response and TCTS score in the Wolf cohort 2021, Ascierto cohort 2016, Homet cohort 2019, and Amato cohort 2020, respectively. E-H. The ROC curves illustrating the prediction performance of TCTS in the Wolf cohort 2021, Ascierto cohort 2016, Homet cohort 2019, and Amato cohort 2020. I-N. The correlation between TCTS and IC50 of oxaliplatin in the TCGA cohort, ICGC cohort, GSE76427 cohort, GSE54236 cohort, GSE27150 cohort and GSE14520 cohort.

Conclusion

We constructed a robust and powerful TCTS based on 95 machine learning integrations using 8 independent clinical cohorts. The TCTS enabled precise assessment of prognosis, and was significantly correlated with clinical indicators and molecular features. Compared with 77 previously published gene signatures, the superior predictive capacity and robust performance of TCTS was established. In the FAHWMU cohort, a novel nomogram (embracing TNM stage, Hepatitis B, vascular invasion, perineural invasion, AFP and TCTS) was constructed to emphasize the clinical applications of TCTS. The high TCTS score group exhibited dismal prognostic outcomes, significant sensitivity to oxaliplatin and immunotherapy. The low TCTS score group was associated with low tumor mutation levels, low immune activations and low PD-1/PD-L1 expressions. In summary, TCTS is an ideal biomarker for informing on the clinical outcomes and precision treatment of HCC.

Acknowledgements

The study was supported by Wenzhou Science and Technology Bureau (grant No. Y20210180 and 2021Y1377) and Zhejiang Provincial Research Centre for Diagnosis and Treatment of Critical Liver and Biliary Diseases (Minimally Invasive).

This study was approved by the research ethics committee of the First Affiliated Hospital of Wenzhou Medical University. All patients gave their informed consent.

Disclosure of conflict of interest

None.

Address correspondence to: Zhenxu Zhou, Department of Hernia and Abdominal Wall Surgery, The First Affiliated Hospital of Wenzhou Medical University, No. 2 Fuxue Lane, Wenzhou, Zhejiang, P. R. China. Tel: +86-577-55579309; Fax: +86-577-55579309; E-mail: zzx750301@163.com; Jianjian Zheng, Key Laboratory of Clinical Laboratory Diagnosis and Translational Research of Zhejiang Province, The First Affiliated Hospital of Wenzhou Medical University, No. 2 Fuxue Lane, Wenzhou, Zhejiang, P. R. China. E-mail: zjj@wmu.edu.cn

References

- [1] Global Burden of Disease Cancer Collaboration; Fitzmaurice C, Allen C, Barber RM, Barre-gard L, Bhutta ZA, Brenner H, Dicker DJ, Chimed-Orchir O, Dandona R, Dandona L, Fleming T, Forouzanfar MH, Hancock J, Hay RJ, Hunter-Merrill R, Huynh C, Hosgood HD, Johnson CO, Jonas JB, Khubchandani J, Kumar GA, Kutz M, Lan Q, Larson HJ, Liang X, Lim SS, Lopez AD, MacIntyre MF, Marczak L, Marquez N, Mokdad AH, Pinho C, Pourmalek F, Salomon JA, Sanabria JR, Sandar L, Sartorius B, Schwartz SM, Shackelford KA, Shibuya K, Stanaway J, Steiner C, Sun J, Takahashi K, Vollset SE, Vos T, Wagner JA, Wang H, Westerman R, Zeeb H, Zoeckler L, Abd-Allah F, Ahmed MB, Alabed S, Alam NK, Aldhahri SF, Alem G, Alemayohu MA, Ali R, Al-Raddadi R, Amare A, Amoako Y, Artaman A, Asayesh H, Atnafu N, Awasthi A, Saleem HB, Barac A, Bedi N, Bensenor I, Berhane A, Bernabé E, Betsu B, Binagwaho A, Boneya D, Campos-Nonato I, Castañeda-Orjuela C, Catalá-López F, Chiang P, Chibueze C, Chitheer A, Choi JY, Cowie B, Damtew S, das Neves J, Dey S, Dharmaratne S, Dhillon P, Ding E, Driscoll T, Ekwueme D, Endries AY, Farvid M, Farzadfar F, Fernandes J, Fischer F, TT GH, Gebru A, Gopalani S, Hailu A, Horino M, Horita N, Hussein A, Huybrechts I, Inoue M, Islami F, Jakovljevic M, James S, Javanbakht M, Jee SH, Kasaeian A, Kedir MS, Khader YS, Khang YH, Kim D, Leigh J, Linn S, Lunevicius R, El Razek HMA, Malekzadeh R, Malta DC, Marcenes W, Markos D, Melaku YA, Meles KG, Mendoza W, Mengiste DT, Meretoja TJ, Miller TR, Mohammad KA, Mohammadi A, Mohammed S, Moradi-Lakeh M, Nagel G, Nand D, Le Nguyen Q, Nolte S, Ogbo FA, Oladimeji KE, Oren E, Pa M, Park EK, Pereira DM, Plass D, Qorbani M, Radfar A, Rafay A, Rahman M, Rana SM, Sørreide K, Satpathy M, Sawhney M, Sepanlou SG, Shaikh MA, She J, Shiue I, Shore HR, Shrimme MG, So S, Soneji S, Stathopoulou V, Stroumpoulis K, Sufiyan MB, Sykes BL, Tabarés-Seisdedos R, Tadese F, Tedla BA, Tessema GA, Thakur JS, Tran BX, Ukwaja KN, Uzochukwu BSC, Vlassov VV, Weiderpass E, Wubshet Terefe M, Yeboyo HG, Yimam HH, Yonemoto N, Younis MZ, Yu C, Zaidi Z, Zaki MES, Zenebe ZM, Murray CJL and Naghavi M. Global, regional, and national cancer incidence, mortality, years of life lost, years lived with disability, and disability-adjusted life-years for 32 cancer groups, 1990 to 2015: a systematic analysis for the global burden of disease study. *JAMA Oncol* 2017; 3: 524-548.
- [2] Yang JD, Hainaut P, Gores GJ, Amadou A, Plym-oth A and Roberts LR. A global view of hepato-

A novel T-cell-tolerance derived signature

- cellular carcinoma: trends, risk, prevention and management. *Nat Rev Gastroenterol Hepatol* 2019; 16: 589-604.
- [3] Calderaro J, Seraphin TP, Luedde T and Simon TG. Artificial intelligence for the prevention and clinical management of hepatocellular carcinoma. *J Hepatol* 2022; 76: 1348-1361.
- [4] Singal AG, Mukherjee A, Elmunzer BJ, Higgins PD, Lok AS, Zhu J, Marrero JA and Waljee AK. Machine learning algorithms outperform conventional regression models in predicting development of hepatocellular carcinoma. *Am J Gastroenterol* 2013; 108: 1723-1730.
- [5] Ioannou GN, Tang W, Beste LA, Tincopa MA, Su GL, Van T, Tapper EB, Singal AG, Zhu J and Waljee AK. Assessment of a deep learning model to predict hepatocellular carcinoma in patients with hepatitis c cirrhosis. *JAMA Netw Open* 2020; 3: e2015626.
- [6] Yang JD and Heimbach JK. New advances in the diagnosis and management of hepatocellular carcinoma. *BMJ* 2020; 371: m3544.
- [7] Singal AG, Pillai A and Tiro J. Early detection, curative treatment, and survival rates for hepatocellular carcinoma surveillance in patients with cirrhosis: a meta-analysis. *PLoS Med* 2014; 11: e1001624.
- [8] Sangro B, Sarobe P, Hervás-Stubbs S and Melero I. Advances in immunotherapy for hepatocellular carcinoma. *Nat Rev Gastroenterol Hepatol* 2021; 18: 525-543.
- [9] Prieto J, Melero I and Sangro B. Immunological landscape and immunotherapy of hepatocellular carcinoma. *Nat Rev Gastroenterol Hepatol* 2015; 12: 681-700.
- [10] Bruix J, Chan S, Galle P, Rimassa L and Sangro B. Systemic treatment of hepatocellular carcinoma: an EASL position paper. *J Hepatol* 2021; 75: 960-974.
- [11] Lyu N, Wang X, Li JB, Lai JF, Chen QF, Li SL, Deng HJ, He M, Mu LW and Zhao M. Arterial chemotherapy of oxaliplatin plus fluorouracil versus sorafenib in advanced hepatocellular carcinoma: a biomolecular exploratory, randomized, phase III trial (FOHAIC-1). *J Clin Oncol* 2022; 40: 468-480.
- [12] Lyu N, Kong Y, Mu L, Lin Y, Li J, Liu Y, Zhang Z, Zheng L, Deng H, Li S, Xie Q, Guo R, Shi M, Xu L, Cai X, Wu P and Zhao M. Hepatic arterial infusion of oxaliplatin plus fluorouracil/leucovorin vs. sorafenib for advanced hepatocellular carcinoma. *J Hepatol* 2018; 69: 60-69.
- [13] Kang YK, Chen LT, Ryu MH, Oh DY, Oh SC, Chung HC, Lee KW, Omori T, Shitara K, Sakamoto S, Chung IJ, Yamaguchi K, Kato K, Sym SJ, Kadowaki S, Tsuji K, Chen J, Bai LY, Oh S, Choda Y, Yasui H, Takeuchi K, Hirashima Y, Hagihara S and Boku N. Nivolumab plus chemotherapy versus placebo plus chemotherapy in patients with HER2-negative, untreated, unresectable advanced or recurrent gastric or gastro-oesophageal junction cancer (ATTRACTION-4): a randomised, multicentre, double-blind, placebo-controlled, phase 3 trial. *Lancet Oncol* 2022; 23: 234-247.
- [14] Michelson DA, Hase K, Kaisho T, Benoist C and Mathis D. Thymic epithelial cells co-opt lineage-defining transcription factors to eliminate autoreactive T cells. *Cell* 2022; 185: 2542-2558, e18.
- [15] Li G, Liu D, Cooper TK, Kimchi ET, Qi X, Avella DM, Li N, Yang QX, Kester M, Rountree CB, Kaifi JT, Cole D, Rockey DC, Schell TD and Staveley-O'Carroll K. Successful chemoimmunotherapy against hepatocellular cancer in a novel murine model. *J Hepatol* 2017; 66: 75-85.
- [16] Yi C, Chen L, Lin Z, Liu L, Shao W, Zhang R, Lin J, Zhang J, Zhu W, Jia H, Qin L, Lu L and Chen J. Lenvatinib targets FGF receptor 4 to enhance antitumor immune response of anti-programmed cell death-1 in HCC. *Hepatology* 2021; 74: 2544-2560.
- [17] Villa E, Critelli R, Lei B, Marzocchi G, Cammà C, Giannelli G, Pontisso P, Cabibbo G, Enea M, Colopi S, Caporali C, Pollicino T, Milosa F, Karampatou A, Todesca P, Bertolini E, Maccio L, Martinez-Chantar ML, Turola E, Del Buono M, De Maria N, Ballestri S, Schepis F, Loria P, Enrico Gerunda G, Losi L and Cillo U. Neoangiogenesis-related genes are hallmarks of fast-growing hepatocellular carcinomas and worst survival. Results from a prospective study. *Gut* 2016; 65: 861-869.
- [18] Grinchuk OV, Yenamandra SP, Iyer R, Singh M, Lee HK, Lim KH, Chow PK and Kuznetsov VA. Tumor-adjacent tissue co-expression profile analysis reveals pro-oncogenic ribosomal gene signature for prognosis of resectable hepatocellular carcinoma. *Mol Oncol* 2018; 12: 89-113.
- [19] Roessler S, Jia HL, Budhu A, Forgues M, Ye QH, Lee JS, Thorgerirsson SS, Sun Z, Tang ZY, Qin LX and Wang XW. A unique metastasis gene signature enables prediction of tumor relapse in early-stage hepatocellular carcinoma patients. *Cancer Res* 2010; 70: 10202-10212.
- [20] Rode I and Rodewald HR. Transcription factor hijacking in the name of tolerance. *Cell* 2022; 185: 2398-2400.
- [21] Wilkerson MD and Hayes DN. ConsensusClusterPlus: a class discovery tool with confidence assessments and item tracking. *Bioinformatics* 2010; 26: 1572-1573.
- [22] Senbabaoğlu Y, Michailidis G and Li J. Critical limitations of consensus clustering in class discovery. *Sci Rep* 2014; 4: 6207.
- [23] Newman AM, Liu CL, Green MR, Gentles AJ, Feng W, Xu Y, Hoang CD, Diehn M and Alizadeh

A novel T-cell-tolerance derived signature

- AA. Robust enumeration of cell subsets from tissue expression profiles. *Nat Methods* 2015; 12: 453-457.
- [24] El-Serag HB and Kanwal F. Epidemiology of hepatocellular carcinoma in the United States: where are we? Where do we go? *Hepatology* 2014; 60: 1767-1775.
- [25] Schlegel A, van Reeve M, Croome K, Parente A, Dolcet A, Widmer J, Meurisse N, De Carlis R, Hessheimer A, Jochmans I, Mueller M, van Leeuwen OB, Nair A, Tomiyama K, Sherif A, Elsharif M, Kron P, van der Helm D, Borja-Cacho D, Bohorquez H, Germanova D, Dondosola D, Olivieri T, Camagni S, Gorgen A, Patrono D, Cescon M, Croome S, Panconesi R, Carvalho MF, Ravaioli M, Caicedo JC, Loss G, Lucidi V, Sapisochin G, Romagnoli R, Jassem W, Colledan M, De Carlis L, Rossi G, Di Benedetto F, Miller CM, van Hoek B, Attia M, Lodge P, Hernandez-Alejandro R, Detry O, Quintini C, Oniscu GC, Fondevila C, Malagó M, Pirenne J, IJzermans JNM, Porte RJ, Dutkowski P, Taner C, Heaton N, Clavien PA, Polak WG and Muiesan P; DCD Collaborator Group. A multicentre outcome analysis to define global benchmarks for donation after circulatory death liver transplantation. *J Hepatol* 2022; 76: 371-382.
- [26] Huitzil-Melendez FD, Capanu M, O'Reilly EM, Duffy A, Gansukh B, Saltz LL and Abou-Alfa GK. Advanced hepatocellular carcinoma: which staging systems best predict prognosis? *J Clin Oncol* 2010; 28: 2889-2895.
- [27] Seo N, Joo DJ, Park MS, Kim SS, Shin HJ, Chung YE, Choi JY, Kim MS and Kim MJ. Optimal imaging criteria and modality to determine Milan criteria for the prediction of post-transplant HCC recurrence after locoregional treatment. *Eur Radiol* 2023; 33: 501-511.
- [28] Aatresh AA, Alabhya K, Lal S, Kini J and Saxena PUP. LiverNet: efficient and robust deep learning model for automatic diagnosis of sub-types of liver hepatocellular carcinoma cancer from H&E stained liver histopathology images. *Int J Comput Assist Radiol Surg* 2021; 16: 1549-1563.
- [29] Li R, Zhao W, Liang R, Jin C and Xiong H. Identification and validation of a novel tumor micro-environment-related prognostic signature of patients with hepatocellular carcinoma. *Front Mol Biosci* 2022; 9: 917839.
- [30] Patel SK, George B and Rai V. Artificial intelligence to decode cancer mechanism: beyond patient stratification for precision oncology. *Front Pharmacol* 2020; 11: 1177.
- [31] Mokrane FZ, Lu L, Vavasseur A, Otal P, Peron JM, Luk L, Yang H, Ammari S, Saenger Y, Rousseau H, Zhao B, Schwartz LH and Dercle L. Radiomics machine-learning signature for diagnosis of hepatocellular carcinoma in cirrhotic patients with indeterminate liver nodules. *Eur Radiol* 2020; 30: 558-570.
- [32] Ma W, Yao Y, Xu G, Wu X, Li J, Wang G, Chen X, Wang K, Chen Y, Guo Y, Li Y, Tan D, Guo H, Liu Z, Yuan Y and Claret FX. Identification of a seven-long non-coding RNA signature associated with Jab1/CSN5 in predicting hepatocellular carcinoma. *Cell Death Discov* 2021; 7: 178.
- [33] Fu J, Qin W, Tong Q, Li Z, Shao Y, Liu Z, Liu C, Wang Z and Xu X. A novel DNA methylation-driver gene signature for long-term survival prediction of hepatitis-positive hepatocellular carcinoma patients. *Cancer Med* 2022; 11: 4721-4735.
- [34] Su L, Zhang G and Kong X. A novel five-gene signature for prognosis prediction in hepatocellular carcinoma. *Front Oncol* 2021; 11: 642563.
- [35] Chen PF, Li QH, Zeng LR, Yang XY, Peng PL, He JH and Fan B. A 4-gene prognostic signature predicting survival in hepatocellular carcinoma. *J Cell Biochem* 2019; 120: 9117-9124.
- [36] Cheng B, Zhou P and Chen Y. Machine-learning algorithms based on personalized pathways for a novel predictive model for the diagnosis of hepatocellular carcinoma. *BMC Bioinformatics* 2022; 23: 248.
- [37] Guo X, Xiong H, Dong S and Wei X. Identification and validation of a novel immune infiltration-based diagnostic score for early detection of hepatocellular carcinoma by machine-learning strategies. *Gastroenterol Res Pract* 2022; 2022: 5403423.
- [38] Lurje I, Hammerich L and Tacke F. Dendritic cell and T cell crosstalk in liver fibrogenesis and hepatocarcinogenesis: implications for prevention and therapy of liver cancer. *Int J Mol Sci* 2020; 21: 7378.
- [39] Chen Y and Tian Z. HBV-induced immune imbalance in the development of HCC. *Front Immunol* 2019; 10: 2048.
- [40] Mossanen JC, Kohlhepp M, Wehr A, Krenkel O, Liepelt A, Roeth AA, Möckel D, Heymann F, Lammers T, Gassler N, Hermann J, Jankowski J, Neumann UP, Luedde T, Trautwein C and Tacke F. CXCR6 inhibits hepatocarcinogenesis by promoting natural killer T- and CD4 T-cell-dependent control of senescence. *Gastroenterology* 2019; 156: 1877-1889, e4.
- [41] Flecken T, Schmidt N, Hild S, Gostick E, Drognitz O, Zeiser R, Schemmer P, Bruns H, Eiermann T, Price D, Blum H, Neumann-Haefelin C and Thimme R. Immunodominance and functional alterations of tumor-associated antigen-specific CD8+ T-cell responses in hepatocellular carcinoma. *Hepatology* 2014; 59: 1415-1426.
- [42] Kikuchi H, Matsui A, Morita S, Amoozgar Z, Inoue K, Ruan Z, Staiculescu D, Wong JS, Huang

A novel T-cell-tolerance derived signature

- P, Yau T, Jain RK and Duda DG. Increased CD8+ T-Cell infiltration and efficacy for multikinase inhibitors after PD-1 blockade in hepatocellular carcinoma. *J Natl Cancer Inst* 2022; 114: 1301-1305.
- [43] Chen J, Lin Z, Liu L, Zhang R, Geng Y, Fan M, Zhu W, Lu M, Lu L, Jia H, Zhang J and Qin LX. GOLM1 exacerbates CD8 T cell suppression in hepatocellular carcinoma by promoting exosomal PD-L1 transport into tumor-associated macrophages. *Signal Transduct Target Ther* 2021; 6: 397.
- [44] Ding ZB, Hui B, Shi YH, Zhou J, Peng YF, Gu CY, Yang H, Shi GM, Ke AW, Wang XY, Song K, Dai Z, Shen YH and Fan J. Autophagy activation in hepatocellular carcinoma contributes to the tolerance of oxaliplatin via reactive oxygen species modulation. *Clin Cancer Res* 2011; 17: 6229-6238.
- [45] Woo H, Wang XW, Budhu A, Kim YH, Kwon SM, Tang ZY, Sun Z, Harris CC and Thorgeirsson SS. Association of TP53 mutations with stem cell-like gene expression and survival of patients with hepatocellular carcinoma. *Gastroenterology* 2011; 140: 1063-1070.

A novel T-cell-tolerance derived signature

Table S1. The clinical characteristics for HCC patients in the FAHWMU cohort

	FAHWMU cohort (n=158)
Age, years	50.66±11.48
Gender	
male	86 (54.4%)
female	72 (45.6%)
TMN stage	
I	52 (32.9%)
II	32 (20.3%)
III	62 (39.2%)
IV	12 (7.6%)
Tumor size, cm	
≤ 5	90 (57.0%)
> 5	68 (43.0%)
Hepatitis B	
negative	84 (53.2%)
positive	74 (46.8%)
Lymph node invasion	
no	114 (72.2%)
yes	44 (27.8%)
Vascular invasion	
no	102 (64.6%)
yes	56 (35.4%)
Perineural invasion	
no	96 (60.8%)
yes	62 (39.2%)
albumin, g/L	40.14±3.52
AFP, ng/ml	2.62±0.32
CEA, ug/L	1.93±0.86
CA199, U/ml	47.57±12.93

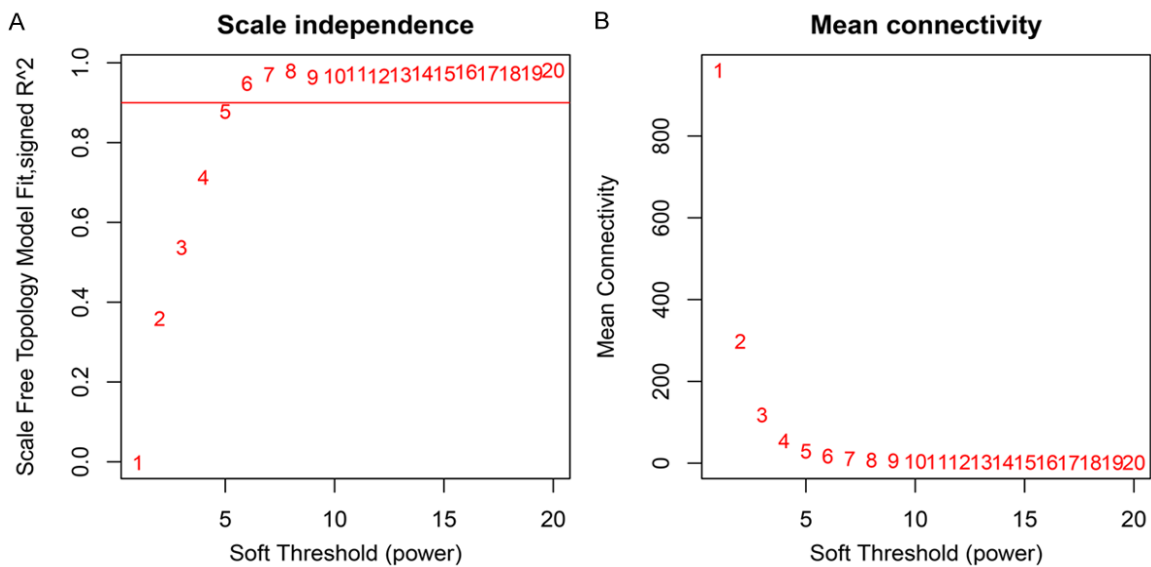


Figure S1. The determination of the optimal soft threshold in the WGCNA analysis. A. The left panel shows the impact of soft-threshold power on the scale-free topology fit index; B. the right panel displays the impact of soft-threshold power on the mean connectivity.

A novel T-cell-tolerance derived signature

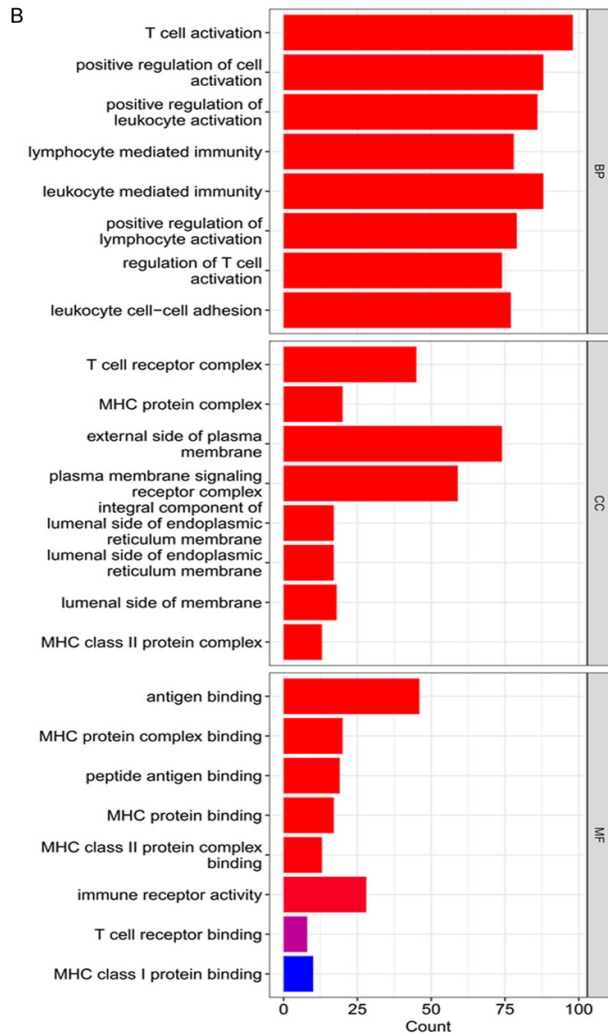
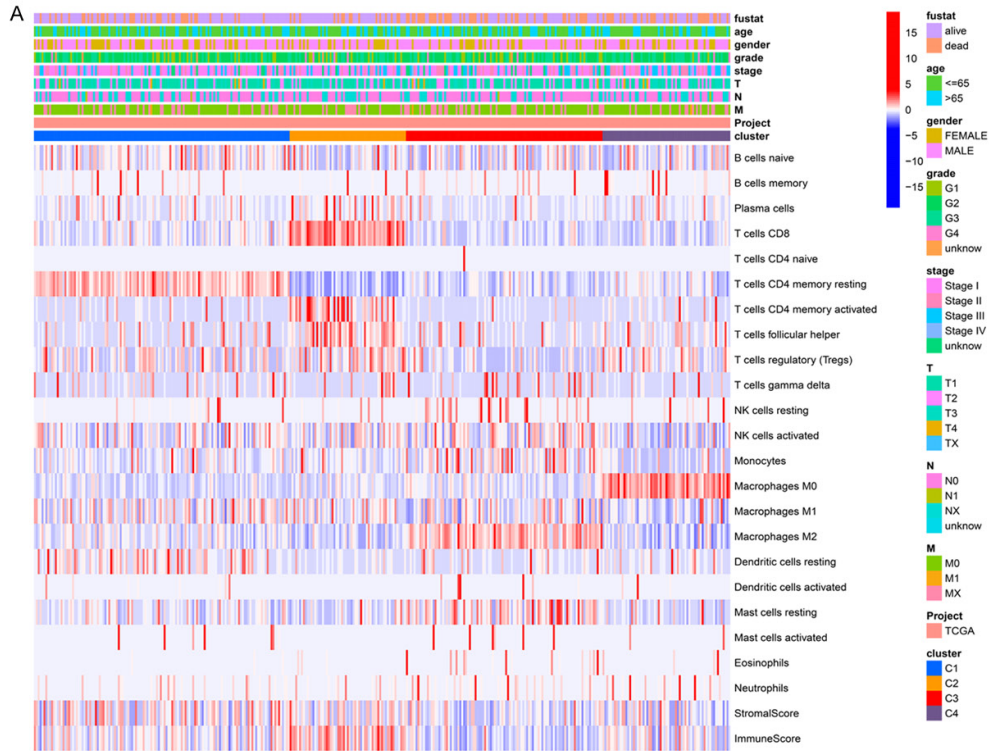


Figure S2. A. The complex heatmap of 22 main TIICs, ESTIMATE scores and clinical characteristics between different TCT related clusters. **B.** GO enrichment analysis demonstrated the significant biological functions in the optimal TCT related pattern.

A novel T-cell-tolerance derived signature

Table S2. The list of 252 intersection genes

Number	Gene	Number	Gene	Number	Gene	Number	Gene
1	MTARC2	71	CCDC137	141	EIF3M	211	C12orf75
2	SERPINA6	72	CSTB	142	TLL12	212	HKDC1
3	BDH1	73	WSB2	143	SMARCD1	213	RTN3
4	CYP2C9	74	ACTG1	144	ENAH	214	G6PD
5	PDE8A	75	MBOAT7	145	PGD	215	B4GALNT4
6	IL1RN	76	CFL1	146	SRC	216	NAE1
7	C3	77	TPGS2	147	TTC39A	217	LYPLA2
8	TMEM220	78	IER3IP1	148	AC245060.4	218	EMC8
9	ALDH8A1	79	PGAM5	149	ERO1A	219	HILPDA
10	HRG	80	YBX1	150	MSANTD3	220	PIP4P2
11	AGXT	81	MTHFD1L	151	UTP4	221	GAL3ST1
12	F2	82	TSPO	152	CD151	222	YTHDF2
13	SEC62	83	CD63	153	DNAJC10	223	PHB
14	PRRG4	84	TM4SF1	154	TMEM184B	224	ZMYND8
15	SHF	85	MACIR	155	DPCD	225	TARS1
16	DCXR	86	TONSL	156	CCNB1	226	TEAD4
17	HMGA1	87	SOX4	157	UCK2	227	RHPN1
18	ENO1	88	BCAR1	158	ARPC1A	228	SKA1
19	ALDOA	89	PRAME	159	CS	229	EWSR1
20	SLC16A3	90	MFSD10	160	CXXC1	230	PLEKHB2
21	CCT6A	91	GARS1	161	SSR3	231	SQSTM1
22	ATIC	92	CCT8	162	SMIM22	232	HSPA4
23	MIR210HG	93	LDHA	163	FKBP9	233	MPZL1
24	KDELR1	94	PPIAP22	164	SMS	234	SLC39A6
25	DBN1	95	SGSM3	165	EPRS1	235	HARS2
26	VDAC1	96	SNRPD1	166	KIAA1522	236	CCDC6
27	MACROH2A1	97	CTNNA1	167	CNOT11	237	ATP6V1E1
28	SAMD10	98	RNF145	168	S100A11	238	MYBL2
29	STIP1	99	RBM38	169	RUVBL1	239	C2CD4A
30	EEF1E1	100	YBX3	170	SOX12	240	PERP
31	GAPDH	101	JPT1	171	ANKRD13D	241	VDAC2
32	NME2	102	CD58	172	CCDC9	242	ANXA2
33	TRIM65	103	MTMR2	173	POPDC3	243	CORO1C
34	ARPC1B	104	RARS1	174	ELOVL1	244	ITGB4
35	GLRX3	105	TPI1	175	VASP	245	AP2A2
36	SYNGR2	106	WDR4	176	DLAT	246	UBE2S
37	RALA	107	DHX37	177	CSNK1E	247	RRP12
38	THOC5	108	LARS1	178	NOL3	248	SEPTIN5
39	DCUN1D5	109	UBE2L3	179	YARS2	249	DENR
40	HMGXB3	110	VPS37C	180	UAP1L1	250	UTP11
41	SLC38A1	111	FBXL19	181	DDA1	251	PABPC4
42	CBX3	112	C12orf49	182	RCC1	252	ZMIZ2
43	NPM1	113	BAK1	183	DNAAF5	253	
44	ATAD3B	114	AKAP8L	184	DDOST	254	
45	TAGLN2	115	TEAD2	185	LPCAT1	255	
46	CYTH2	116	FARSB	186	ANO9	256	
47	SMOX	117	CCT5	187	RIT1	257	
48	SPAG4	118	NAP1L1	188	PTTG1IP	258	
49	RAN	119	TBC1D22A	189	TNFRSF12A	259	

A novel T-cell-tolerance derived signature

50	TRIP10	120	BMS1	190	KPNA2	260
51	CCT2	121	PHF5A	191	MICALL2	261
52	STX3	122	PAFAH1B2	192	MARS1	262
53	PLPP2	123	LAPTM4B	193	ARHGEF2	263
54	OLA1	124	DLGAP4	194	PDSS1	264
55	SPATS2	125	SPHK1	195	TMED3	265
56	PITX1	126	TCOF1	196	SAE1	266
57	PRR7	127	RCC2	197	ITGA2	267
58	B4GALT2	128	MRT04	198	TCF3	268
59	PLXNA3	129	MAST2	199	GPN2	269
60	PRXL2B	130	CEBPZOS	200	PTGFRN	270
61	NLE1	131	RANGAP1	201	NOP58	271
62	AP4M1	132	FAM241B	202	KDM1A	272
63	BTF3L4	133	HOMER3	203	NCBP2	273
64	NARS1	134	PHLDA2	204	RANBP1	274
65	ZDHHC7	135	IFNGR2	205	WDR45B	275
66	MEX3A	136	CD24	206	MMP9	276
67	EIF3D	137	NCDN	207	MCRS1	277
68	GNPDA1	138	ETF1	208	RPN2	278
69	NPAS2	139	NRSN2	209	PRPF19	279
70	BZW2	140	FHL3	210	TXNDC12	280

Table S3. The details of 77 published gene risk signatures used in this study

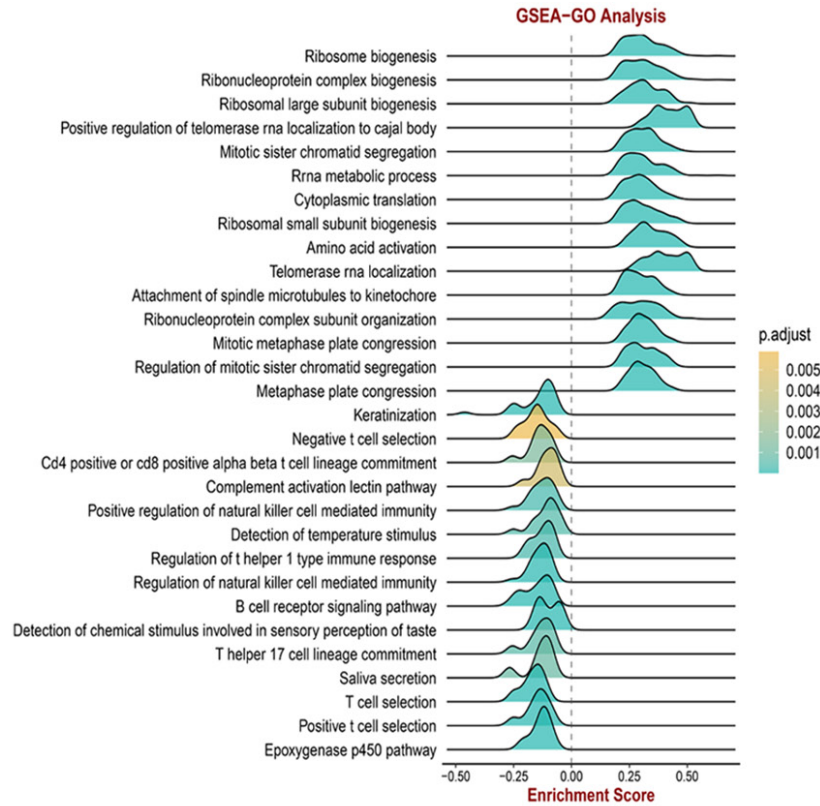
Signatures	Authors
Recurrence associated immune gene signature	Chen Y [1]
pyroptosis-related lncRNAs signature	Liu Z [2]
Pyroptosis-related gene signature	Zhang S [3]
Amino acid metabolism-related signature	Zhao Y [4]
Microvascular invasion related signature	Du B [5]
Four-gene signature	Liu J [6]
Hypoxia gene signature	Zhang Q [7]
FR-lncRNAs signature	Zhang Z [8]
Costimulatory molecule gene signature	Hu Y [9]
Hypoxia-associated lncRNAs signature	Chang M [10]
Epithelial-mesenchymal transition-related 5-gene signature	Zhu G [11]
Prognostic and therapeutic immune signature	Peng Y [12]
Instability-associated lncRNAs signature	Yan Y [13]
EMT-related lncRNAs signature	Tao H [14]
Metabolism-related gene signature	Yuan C [15]
N6-methyladenosine-associated prognostic signature	Zhu P [16]
Metabolism-related signature	Wang Z [17]
Seven-gene signature	Xie H [18]
Cell cycle progression-derived gene signature	Hui Y [19]
Immune-related risk signature	Liu Z [20]
PPAR-related multigene signature	Xu W [21]
Metabolism-related lncRNAs signature	Wang W [22]
TME-related lncRNAs signature	Huang S [23]
Ubiquitin-specific proteases related signature	Ni W [24]
Toll-like receptor-based gene signature	Liu L [25]
Glycolysis-related gene signature	Yang J [26]
Ahypoxia-related signature	Jiang H [27]

A novel T-cell-tolerance derived signature

Five-gene signature	Su L [28]
4-gene prognostic signature	Chen P [29]
m6A regulator-related LncRNAs signature	Jin C [30]
Mutational burden-associated LncRNA signature	Xu M [31]
Six-gene signature	Liu G [32]
Tumor microenvironment-related gene signature	Huang C [33]
Immune checkpoint-related gene signature	Zhao E [34]
Glycolysis-related gene signature	Zhou W [35]
Pyroptosis-related gene signature	He J [36]
Three-gene signature derived from AATF coexpressed genes	Liu J [37]
IAR-lncRNA signature	Wang Y [38]
Immune-related lncRNA signature	Deng M [39]
HCC-specific gene transcriptional signature	Petrizzo A [40]
mTORC1 pathway derived signature	Mo Z [41]
SVM based signature	Yerukala S [42]
Necroptosis-related gene signature	Chen J [43]
Hypoxia-related lncRNAs signature	Tang P [44]
Immune- and Ferroptosis-related LncRNA signature	Huang A [45]
Mutation-related lncRNAs signature	Wu J [46]
Stemness-based eleven-gene signature	Hong L [47]
14-gene signature	Zhang B [48]
Tumor doubling time-related immune gene signature	Zhang G [49]
Hypoxia-driven gene signature	Zeng Z [50]
Liver progenitor cell-related genes signature	Li X [51]
Inflammatory response-related gene signature	Lin Z [52]
HBV-related lncRNAs signature	Nong S [53]
Hypoxia-related lncRNA signature	Zhou C [54]
Somatic mutation-derived LncRNA signature	Guo C [55]
m6A-related signature	Jiang H [56]
Cell cycle-related 13-mRNA signature	Zhou Y [57]
Metabolic ten-gene signature	Zhu Z [58]
Six-gene-based prognostic signature	Wang Z [59]
Seven-senescence-associated gene signature	Xiang X [59]
Jab1/CSN5 derived LncRNAs signature	Ma W [60]
m6A methyltransferase-related lncRNA signature	Li L [61]
Autophagy-related lncRNAs signature	Wu H [62]
Immune-related lncRNA signature	Kong W [63]
Five-CpG-based prognostic signature	Fang F [64]
DNA methylation-driver gene signature	Fu J [65]
Glycosyltransferase prognostic signature	Zhou Z [66]
Ferroptosis-related gene signature	Wang H [67]
Four-methylated lncRNAs-based prognostic signature	Liao L [68]
9-long non-coding RNA signature	Deng B [69]
Four-long noncoding RNA signature	Jiang H [70]
Hypoxia-related signature	Zhang B [71]
Non-apoptotic programmed cell death-related gene signature	Zhang G [72]
Pseudogene pair-based prognostic signature	Du Y [73]
Lipid metabolism-related and immune-associated prognostic signature	Hu B [74]
Metabolic gene-based prognostic signature	Weng J [75]
Eight-lncRNA prognostic signature	Zhao X [76]
Autophagy-related lncRNA signature	Yang S [77]

A novel T-cell-tolerance derived signature

A



B

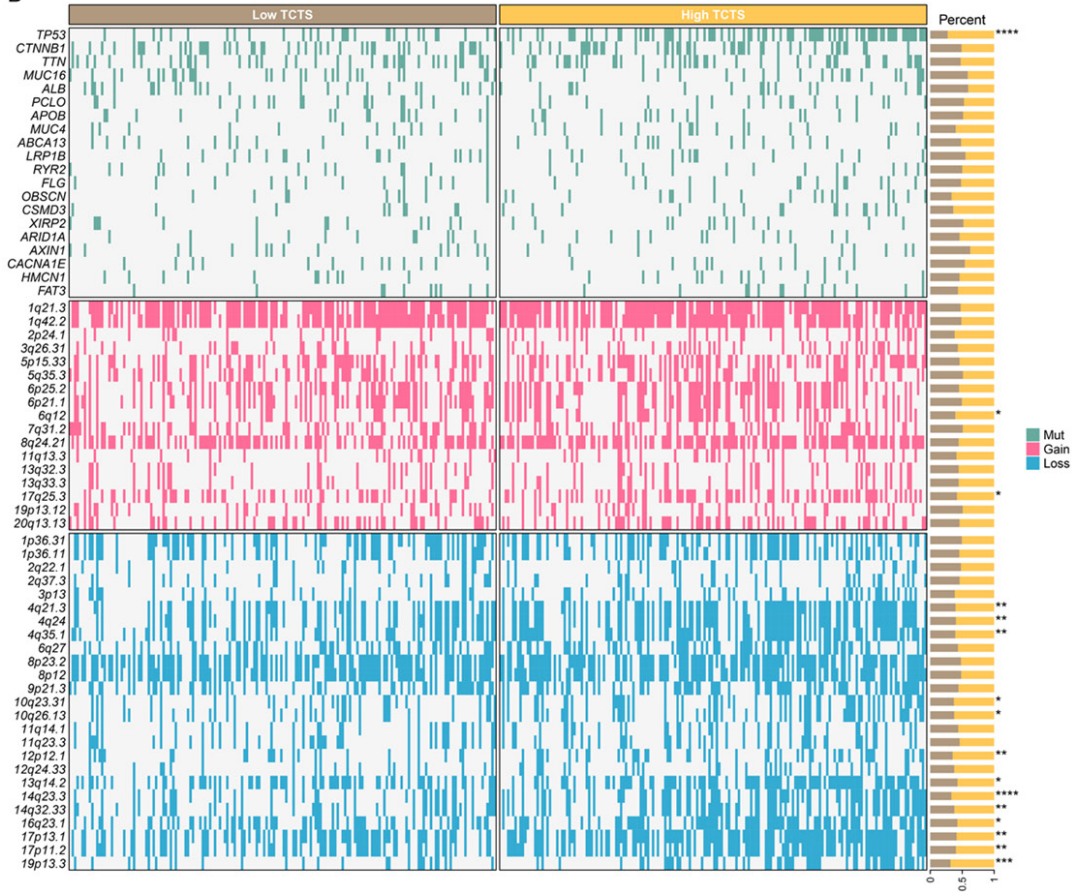


Figure S3. A. The GSEA-GO analysis displayed the remarkable biological pathways enriched according to the difference of TCTS. B. The heatmap showed the distribution of genomic alteration between Low- and High-TCTS groups (*: $P < 0.05$; **: $P < 0.01$; ***: $P < 0.001$; ****: $P < 0.0001$).

A novel T-cell-tolerance derived signature

References

- [1] Chen Y, Guo Z, Zeng Y, Su H, Zhong F, Jiang K and Yuan G. A novel recurrence associated immune gene signature and its clinical significance in liver cancer. *Am J Transl Res* 2021; 13: 8766-76.
- [2] Liu ZK, Wu KF, Zhang RY, Kong LM, Shang RZ, Lv JJ, Li C, Lu M, Yong YL, Zhang C, Zheng NS, Li YH, Chen ZN, Bian H and Wei D. Pyroptosis-related LncRNA signature predicts prognosis and is associated with immune infiltration in hepatocellular carcinoma. *Front Oncol* 2022; 12: 794034.
- [3] Zhang S, Li X, Zhang X, Zhang S, Tang C and Kuang W. The pyroptosis-related gene signature predicts the prognosis of hepatocellular carcinoma. *Front Mol Biosci* 2021; 8: 781427.
- [4] Zhao Y, Zhang J, Wang S, Jiang Q and Xu K. Identification and validation of a nine-gene amino acid metabolism-related risk signature in HCC. *Front Cell Dev Biol* 2021; 9: 731790.
- [5] Du B, Wang F, Jarad B, Wang Z and Zhang Y. A novel signature based on microvascular invasion predicts the recurrence of HCC. *J Transl Med* 2020; 18: 272.
- [6] Liu J, Zhang SQ, Chen J, Li ZB, Chen JX, Lu QQ, Han YS, Dai W, Xie C and Li JC. Identifying prognostic significance of RCL1 and four-gene signature as novel potential biomarkers in HCC patients. *J Oncol* 2021; 2021: 5574150.
- [7] Zhang Q, Qiao L, Liao J, Liu Q, Liu P and Liu L. A novel hypoxia gene signature indicates prognosis and immune microenvironments characters in patients with hepatocellular carcinoma. *J Cell Mol Med* 2021; 25: 3772-84.
- [8] Zhang Z, Zhang W, Wang Y, Wan T, Hu B, Li C, Ge X and Lu S. Construction and validation of a ferroptosis-related lncRNA signature as a novel biomarker for prognosis, immunotherapy and targeted therapy in hepatocellular carcinoma. *Front Cell Dev Biol* 2022; 10: 792676.
- [9] Hu Y, Liu J, Yu J, Yang F, Zhang M, Liu Y, Ma S, Zhou X, Wang J and Han Y. Identification and validation a co-stimulatory molecule gene signature to predict the prognosis and immunotherapy response for hepatocellular carcinoma. *Cancer Cell Int* 2022; 22: 97.
- [10] Cheng M, Zhang J, Cao PB and Zhou GQ. Prognostic and predictive value of the hypoxia-associated long non-coding RNA signature in hepatocellular carcinoma. *Yi Chuan* 2022; 44: 153-67.
- [11] Zhu G, Xia H, Tang Q and Bi F. An epithelial-mesenchymal transition-related 5-gene signature predicting the prognosis of hepatocellular carcinoma patients. *Cancer Cell Int* 2021; 21: 166.
- [12] Peng Y, Liu C, Li M, Li W, Zhang M, Jiang X, Chang Y, Liu L, Wang F and Zhao Q. Identification of a prognostic and therapeutic immune signature associated with hepatocellular carcinoma. *Cancer Cell Int* 2021; 21: 98.
- [13] Yan Y, Ren L, Liu Y and Liu L. Development and validation of genome instability-associated lncRNAs to predict prognosis and immunotherapy of patients with hepatocellular carcinoma. *Front Genet* 2021; 12: 763281.
- [14] Tao H, Zhang Y, Yuan T, Li J, Liu J, Xiong Y, Zhu J, Huang Z, Wang P, Liang H and Zhang E. Identification of an EMT-related lncRNA signature and LINC01116 as an immune-related oncogene in hepatocellular carcinoma. *Aging (Albany NY)* 2022; 14: 1473-91.
- [15] Yuan C, Yuan M, Chen M, Ouyang J, Tan W, Dai F, Yang D, Liu S, Zheng Y, Zhou C and Cheng Y. Prognostic implication of a novel metabolism-related gene signature in hepatocellular carcinoma. *Front Oncol* 2021; 11: 666199.
- [16] Zhu P, Ren Q, He N, Zhou C, Jin Q and Gong Z. Construction and validation of an N6-methyladenosine-associated prognostic signature in hepatocellular carcinoma. *Oncol Lett* 2021; 21: 221.
- [17] Wang Z, Embaye KS, Yang Q, Qin L, Zhang C, Liu L, Zhan X, Zhang F, Wang X and Qin S. A novel metabolism-related signature as a candidate prognostic biomarker for hepatocellular carcinoma. *J Hepatocell Carcinoma* 2021; 8: 119-32.
- [18] Xie H, Liu S, Zhang Z, Chen P and Tao Y. A novel seven-gene signature as prognostic biomarker in hepatocellular carcinoma. *J Cancer* 2020; 11: 5768-81.
- [19] Hui Y, Leng J, Jin D, Liu D, Wang G, Wang Q and Wang Y. A cell cycle progression-derived gene signature to predict prognosis and therapeutic response in hepatocellular carcinoma. *Dis Markers* 2021; 2021: 1986159.
- [20] Liu Z, Jiao D, Liu L, Zhou X, Yao Y, Li Z, Li J, Chen J, Lei Q and Han X. Development and validation of a robust immune-related risk signature for hepatocellular carcinoma. *Medicine* 2021; 100: e24683.
- [21] Xu W, Chen Z, Liu G, Dai Y, Xu X, Ma D and Liu L. Identification of a potential PPAR-related multigene signature predicting prognosis of patients with hepatocellular carcinoma. *PPAR Res* 2021; 2021: 6642939.
- [22] Wang W, Deng Z, Jin Z, Wu G, Wang J, Zhu H, Xu B, Wen Z and Guo Y. Bioinformatics analysis and experimental verification of five metabolism-related lncRNAs as prognostic models for hepatocellular carcinoma. *Medicine* 2022; 101: e28694.
- [23] Huang S, Zhang J, Lai X, Zhuang L and Wu J. Identification of novel tumor microenvironment-related long non-coding rnas to determine the prognosis and response to immunotherapy of hepatocellular carcinoma patients. *Front Mol Biosci* 2021; 8: 781307.
- [24] Ni W, Bian S, Zhu M, Song Q, Zhang J, Xiao M and Zheng W. Identification and validation of ubiquitin-specific proteases as a novel prognostic signature for hepatocellular carcinoma. *Front Oncol* 2021; 11: 629327.

A novel T-cell-tolerance derived signature

- [25] Liu L, Liu B, Yu J, Zhang D, Shi J and Liang P. Development of a toll-like receptor-based gene signature that can predict prognosis, tumor microenvironment, and chemotherapy response for hepatocellular carcinoma. *Front Mol Biosci* 2021; 8: 729789.
- [26] Yang J, Zhang Y, Duan J, Huang X, Yu H and Hu Z. A glycolysis-related gene signature correlates with the characteristics of the tumor immune microenvironment and predicts prognosis in patients with hepatocellular carcinoma. *Front Mol Biosci* 2022; 9: 834976.
- [27] Jiang HY, Ning G, Wang YS and Lv WB. Ahypoxia-related signature enhances the prediction of the prognosis in hepatocellular carcinoma patients and correlates with sorafenib treatment response. *Am J Transl Res* 2020; 12: 7762-81.
- [28] Su L, Zhang G and Kong X. A novel five-gene signature for prognosis prediction in hepatocellular carcinoma. *Front Oncol* 2021; 11: 642563.
- [29] Chen PF, Li QH, Zeng LR, Yang XY, Peng PL, He JH and Fan B. A 4-gene prognostic signature predicting survival in hepatocellular carcinoma. *J Cell Biochem* 2019; 120: 9117-24.
- [30] Jin C, Li R, Deng T, Li J, Yang Y, Li H, Chen K, Xiong H, Chen G and Wang Y. Identification and validation of a prognostic prediction model of m6a regulator-related LncRNAs in hepatocellular carcinoma. *Front Mol Biosci* 2021; 8: 784553.
- [31] Xu M, Ma T, Shi S, Xing J and Xi Y. Development and validation of a mutational burden-associated LncRNA signature for improving the clinical outcome of hepatocellular carcinoma. *Life (Basel)* 2021; 11: 1312.
- [32] Liu GM, Zeng HD, Zhang CY and Xu JW. Identification of a six-gene signature predicting overall survival for hepatocellular carcinoma. *Cancer Cell Int* 2019; 19: 138.
- [33] Huang C, Zhang C, Sheng J, Wang D, Zhao Y, Qian L, Xie L and Meng Z. Identification and validation of a tumor microenvironment-related gene signature in hepatocellular carcinoma prognosis. *Front Genet* 2021; 12: 717319.
- [34] Zhao E, Chen S and Dang Y. Development and external validation of a novel immune checkpoint-related gene signature for prediction of overall survival in hepatocellular carcinoma. *Front Mol Biosci* 2020; 7: 620765.
- [35] Zhou W, Zhang S, Cai Z, Gao F, Deng W, Wen Y, Qiu ZW, Hou ZK and Chen XL. A glycolysis-related gene pairs signature predicts prognosis in patients with hepatocellular carcinoma. *PeerJ* 2020; 8: e9944.
- [36] He J, Ran J, Li J and Chen D. Construction and validation of a pyroptosis-related gene signature in hepatocellular carcinoma based on RNA sequencing. *Transl Cancer Res* 2022; 11: 1510-22.
- [37] Liu J, Lu J, Ma Z and Li W. A nomogram based on a three-gene signature derived from AATF coexpressed genes predicts overall survival of hepatocellular carcinoma patients. *Biomed Res Int* 2020; 2020: 7310768.
- [38] Wang Y, Ge F, Sharma A, Rudan O, Setiawan MF, Gonzalez-Carmona MA, Kornek MT, Strassburg CP, Schmid M and Schmidt-Wolf IGH. Immunoautophagy-related long noncoding RNA (IAR-lncRNA) signature predicts survival in hepatocellular carcinoma. *Biology* 2021; 10: 1301.
- [39] Deng M, Lin JB, Zhao RC, Li SH, Lin WP, Zou JW, Wei W and Wei W. Construction of a novel immune-related lncRNA signature and its potential to predict the immune status of patients with hepatocellular carcinoma. *BMC Cancer* 2021; 21: 1347.
- [40] Petrizzo A, Caruso FP, Tagliamonte M, Tornesello ML, Ceccarelli M, Costa V, Aprile M, Esposito R, Ciliberto G, Buonaguro FM and Buonaguro L. Identification and validation of HCC-specific gene transcriptional signature for tumor antigen discovery. *Sci Rep* 2016; 6: 29258.
- [41] Mo Z, Zhang S and Zhang S. A novel signature based on mTORC1 pathway in hepatocellular carcinoma. *J Oncol* 2020; 2020: 8291036.
- [42] Yerukala Sathipati S and Ho SY. Novel miRNA signature for predicting the stage of hepatocellular carcinoma. *Sci Rep* 2020; 10: 14452.
- [43] Chen J, Wang H, Zhou L, Liu Z, Chen H and Tan X. A necroptosis-related gene signature for predicting prognosis, immune landscape, and drug sensitivity in hepatocellular carcinoma. *Cancer Med* 2022; 11: 5079-5096.
- [44] Tang P, Qu W, Wang T, Liu M, Wu D, Tan L and Zhou H. Identifying a hypoxia-related long non-coding RNAs signature to improve the prediction of prognosis and immunotherapy response in hepatocellular carcinoma. *Front Genet* 2021; 12: 785185.
- [45] Huang A, Li T, Xie X and Xia J. Computational identification of immune- and ferroptosis-related LncRNA signature for prognosis of hepatocellular carcinoma. *Front Mol Biosci* 2021; 8: 759173.
- [46] Wu J, Ren X, Wang N, Zhou R, Chen M, Cai Y, Lin S, Zhang H, Xie X, Dang C, Zhang S and Zhou Z. A mutation-related long noncoding RNA signature of genome instability predicts immune infiltration and hepatocellular carcinoma prognosis. *Front Genet* 2021; 12: 779554.
- [47] Hong L, Zhou Y, Xie X, Wu W, Shi C, Lin H and Shi Z. A stemness-based eleven-gene signature correlates with the clinical outcome of hepatocellular carcinoma. *BMC Cancer* 2021; 21: 716.
- [48] Zhang BH, Yang J, Jiang L, Lyu T, Kong LX, Tan YF, Li B, Zhu YF, Xi AY, Xu X, Yan LN and Yang JY. Development and validation of a 14-gene signature for prognosis prediction in hepatocellular carcinoma. *Genomics* 2020; 112: 2763-71.

A novel T-cell-tolerance derived signature

- [49] Zhang G, Su L, Lv X and Yang Q. A novel tumor doubling time-related immune gene signature for prognosis prediction in hepatocellular carcinoma. *Cancer Cell Int* 2021; 21: 522.
- [50] Zeng Z, Lei S, Wang J, Yang Y, Lan J, Tian Q, Chen T and Hao X. A novel hypoxia-driven gene signature that can predict the prognosis of hepatocellular carcinoma. *Bioengineered* 2022; 13: 12193-210.
- [51] Li X, Lin J, Pan Y, Cui P and Xia J. Identification of a liver progenitor cell-related genes signature predicting overall survival for hepatocellular carcinoma. *Technol Cancer Res Treat* 2021; 20: 15330338211041425.
- [52] Lin Z, Xu Q, Miao D and Yu F. An inflammatory response-related gene signature can impact the immune status and predict the prognosis of hepatocellular carcinoma. *Front Oncol* 2021; 11: 644416.
- [53] Nong S, Chen X, Wang Z, Xu G, Wei W, Peng B, Zhou L, Wei L, Zhao J, Wei Q, Deng Y and Meng L. Potential lncRNA biomarkers for HBV-related hepatocellular carcinoma diagnosis revealed by analysis on coexpression network. *Biomed Res Int* 2021; 2021: 9972011.
- [54] Zhou C, Zhang H and Lu L. Identification and validation of hypoxia-related lncRNA signature as a prognostic model for hepatocellular carcinoma. *Front Genet* 2021; 12: 744113.
- [55] Guo C, Zhou J, Ma B, Wang R, Ge Y, Wang Z, Ji B, Wang W, Zhang J and Wang Z. A somatic mutation-derived lncRNA signature of genomic instability predicts prognosis for patients with liver cancer. *Front Surg* 2021; 8: 724792.
- [56] Jiang H, Ning G, Wang Y and Lv W. Identification of an m6A-related signature as biomarker for hepatocellular carcinoma prognosis and correlates with sorafenib and Anti-PD-1 immunotherapy treatment response. *Dis Markers* 2021; 2021: 5576683.
- [57] Zhou Y, Lei D, Hu G and Luo F. A cell cycle-related 13-mRNA signature to predict prognosis in hepatocellular carcinoma. *Front Oncol* 2022; 12: 760190.
- [58] Zhu Z, Li L, Xu J, Ye W, Chen B, Zeng J and Huang Z. Comprehensive analysis reveals a metabolic ten-gene signature in hepatocellular carcinoma. *PeerJ* 2020; 8: e9201.
- [59] Wang Z, Teng D, Li Y, Hu Z, Liu L and Zheng H. A six-gene-based prognostic signature for hepatocellular carcinoma overall survival prediction. *Life Sci* 2018; 203: 83-91.
- [60] Ma W, Yao Y, Xu G, Wu X, Li J, Wang G, Chen X, Wang K, Chen Y, Guo Y, Li Y, Tan D, Guo H, Liu Z, Yuan Y and Claret FX. Identification of a seven-long non-coding RNA signature associated with Jab1/CSN5 in predicting hepatocellular carcinoma. *Cell Death Discov* 2021; 7: 178.
- [61] Li L, Xie R and Lu G. Identification of m6A methyltransferase-related lncRNA signature for predicting immunotherapy and prognosis in patients with hepatocellular carcinoma. *Biosci Rep* 2021; 41: BSR20210760.
- [62] Wu H, Liu T, Qi J, Qin C and Zhu Q. Four autophagy-related lncRNAs predict the prognosis of HCC through co-expression and ceRNA mechanism. *Biomed Res Int* 2020; 2020: 3801748.
- [63] Kong W, Wang X, Zuo X, Mao Z, Cheng Y and Chen W. Development and validation of an immune-related lncRNA signature for predicting the prognosis of hepatocellular carcinoma. *Front Genet* 2020; 11: 1037.
- [64] Fang F, Wang X and Song T. Five-CpG-based prognostic signature for predicting survival in hepatocellular carcinoma patients. *Cancer Biol Med* 2018; 15: 425-33.
- [65] Fu J, Qin W, Tong Q, Li Z, Shao Y, Liu Z, Liu C, Wang Z and Xu X. A novel DNA methylation-driver gene signature for long-term survival prediction of hepatitis-positive hepatocellular carcinoma patients. *Cancer Med* 2022; 11: 4721-4735.
- [66] Zhou Z, Wang T, Du Y, Deng J, Gao G and Zhang J. Identification of a novel glycosyltransferase prognostic signature in hepatocellular carcinoma based on LASSO algorithm. *Front Genet* 2022; 13: 823728.
- [67] Wang H, Yang C, Jiang Y, Hu H, Fang J and Yang F. A novel ferroptosis-related gene signature for clinically predicting recurrence after hepatectomy of hepatocellular carcinoma patients. *Am J Cancer Res* 2022; 12: 1995-2011.
- [68] Liao L, Hu D and Zheng Y. A four-methylated lncRNAs-based prognostic signature for hepatocellular carcinoma. *Genes (Basel)* 2020; 11: 908.
- [69] Deng B, Yang M, Wang M and Liu Z. Development and validation of 9-long Non-coding RNA signature to predicting survival in hepatocellular carcinoma. *Medicine* 2020; 99: e20422.
- [70] Jiang H, Zhao L, Chen Y and Sun L. A four-long noncoding RNA signature predicts survival of hepatocellular carcinoma patients. *J Clin Lab Anal* 2020; 34: e23377.
- [71] Zhang B, Tang B, Gao J, Li J, Kong L and Qin L. A hypoxia-related signature for clinically predicting diagnosis, prognosis and immune microenvironment of hepatocellular carcinoma patients. *J Transl Med* 2020; 18: 342.
- [72] Zhang G, Fan W, Wang H, Wen J, Tan J, Xue M and Li J. Non-apoptotic programmed cell death-related gene signature correlates with stemness and immune status and predicts the responsiveness of transarterial chemoembolization in hepatocellular carcinoma. *Front Cell Dev Biol* 2022; 10: 844013.
- [73] Du Y and Gao Y. Development and validation of a novel pseudogene pair-based prognostic signature for prediction of overall survival in patients with hepatocellular carcinoma. *BMC Cancer* 2020; 20: 887.
- [74] Hu B, Yang X and Sang X. Construction of a lipid metabolism-related and immune-associated prognostic signature for hepatocellular carcinoma. *Cancer Med* 2020; 9: 7646-62.

A novel T-cell-tolerance derived signature

- [75] Weng J, Zhou C, Zhou Q, Chen W, Yin Y, Atyah M, Dong Q, Shi Y and Ren N. Development and validation of a metabolic gene-based prognostic signature for hepatocellular carcinoma. *J Hepatocell Carcinoma* 2021; 8: 193-209.
- [76] Zhao X, Bai Z, Li C, Sheng C and Li H. Identification of a novel eight-lncRNA prognostic signature for HBV-HCC and analysis of their functions based on coexpression and ceRNA networks. *Biomed Res Int* 2020; 2020: 8765461.
- [77] Yang S, Zhou Y, Zhang X, Wang L, Fu J, Zhao X and Yang L. The prognostic value of an autophagy-related lncRNA signature in hepatocellular carcinoma. *BMC Bioinformatics* 2021; 22: 217.